Pessimistic Evasive Flow Capturing Problems

Aigerim Bogyrbayeva and Changhyun Kwon*

Department of Industrial and Management Systems Engineering, University of South Florida, Tampa, FL, 33620

October 31, 2020

Abstract

The evasive flow capturing problem (EFCP) is to locate a set of law enforcement facilities to intercept unlawful flows. One application of the EFCP is the location problem of weigh-in-motion systems deployed by authorities to detect overloaded vehicles characterized by evasive behavior. In contrast to the existing literature, this study focuses on the bounded-rationality of drivers and represents the most generic form of the EFCP. We present two pessimistic formulations of the problem to capture various degrees of ambiguity in the route choice of drivers. In particular, we look at the worst-case scenario, when drivers select roads with the highest damage costs. The resulting formulations yield a robust network design and represent the realistic behavior of drivers. The pessimistic formulations introduce another level in the optimization problem, for which we propose a cutting plane algorithm. The proposed solution methods demonstrate their effectiveness on real and randomly generated networks. We also provide numerical analysis to measure the value of considering pessimistic formulations and demonstrate the vulnerability of optimizing and optimistic assumptions on the behavior of drivers.

Keywords: transportation; bilevel optimization; pessimistic formulation; mixed-integer program; cutting plane algorithm

1 Introduction

In this study we consider the pessimistic formulations for the Evasive Flow Capturing Problem (EFCP), defined as to locate law enforcement facilities to intercept unlawful flows. One application of the EFCP is the location of weigh-in-motion systems deployed by authorities to detect overloaded vehicles. Due to considerable risks associated with overloaded vehicles to the road network including threats to traffic safety and damage to infrastructure (Dey et al., 2014), weigh-in-motion (WIM) systems have been employed across the globe and have shown effectiveness in detecting unlawful travelers (Martin et al., 2014; Lu et al., 2002). However, high costs of the WIM stations, which may range between \$30–\$70 thousands per year-lane including installation, maintenance and calibration

---
*Corresponding author: `chkwon@usf.edu`

costs (Szary et al., 2009), prevent them from covering the entire network. At the same time, empirical studies show that truck drivers quickly learn the locations of WIM stations and try to bypass them (Cottrell et al., 1992; Cunagin et al., 1997), highlighting the evasive behavior. Even though it is particularly difficult to eliminate such non-cooperative behavior of drivers, the EFCP aims to locate law enforcement facilities considering these practices. Other applications of the EFCP include the location of safety checkpoints, inspection stations, and tollbooths (Marković et al., 2017).

As a class of Flow Capturing Problems (Hodgson, 1990; Berman et al., 1992), the EFCP is formulated to capture flows of travelers between origin-destination pairs by locating law enforcement facilities (Marković et al., 2015). While in classical flow capturing problems, travelers are assumed to be indifferent to locations of facilities (Yang and Zhou, 1998; Hodgson et al., 1996), in the EFCP, travelers try to bypass them. Therefore, classical assumptions such as the shortest path between origin-destination pairs (Song and Shen, 2016) or fixed paths used to model route choice of travelers are no longer applicable. Indeed, the EFCP is modeled using a deviation tolerance, that accounts for travelers' willingness to deviate from the shortest path so as not to be captured by authorities. First introduced in Berman et al. (1995), deviation paths capture more realistic behavior of drivers (Kim and Kuby, 2012), especially when they are equipped with mobile applications such as Drivewize to advise circumventing routes.

The EFCP is typically studied as a leader-follower game using the corresponding bilevel optimization formulations (Arslan et al., 2018; Hooshmand and MirHassani, 2018; Lu et al., 2017). In this setting, the government is a leader determining the location of law enforcement facilities, and travelers are followers selecting their choices of paths based on the decision of the government, which is typically assumed to be the shortest unintercepted path within a deviation tolerance. In this sense, the EFCP is related to the network design problem in hazardous materials (hazmat) transportation, where the government prohibits hazmat carriers from traveling on certain road segments and hazmat carriers detour accordingly (Kara and Verter, 2004; Gzara, 2013; Sun et al., 2015; Fontaine and Minner, 2018; Fontaine et al., 2020; Su and Kwon, 2020). The main difference is that followers in the EFCP have an option to cancel the travel if there is no path within the deviation tolerance, while followers in the hazmat network design problem always travel regardless of the path length increase.

In the literature of the EFCP, when there are multiple optimal solutions for followers in the lower-level, friendly or optimistic behavior of followers are assumed. Such assumptions on the optimizing behavior of travelers and the optimistic approach in deriving solutions may be appropriate in certain circumstances; however, it does not represent the most general case of the EFCP. Moreover, such an optimistic approach may lead to less desirable solutions, especially when followers are not optimizing decision-makers as we show in our numerical experiments.

In this study, we present the pessimistic formulations of the EFCP to represent the most general case by considering two different perspectives. First, we relax the optimizing behavior by letting travelers select any unintercepted path within a deviation tolerance. This approach is to consider

boundedly rational or satisficing travelers, who select any path whose distance is within a certain threshold of the shortest path (Mahmassani and Chang, 1987; Sun et al., 2018). In fact, empirical studies focused on drivers' choice of routes and network behavior show limitations of the assumptions regarding the rationality of drivers (Nakayama et al., 2001; Zhu and Levinson, 2015). Drivers may be interested in minimizing their travel times, which vary with congestion along routes. In addition, fuel-consumption-aware drivers may have different travel cost evaluations in each route, depending on their exact vehicle type, load weight, and fuel efficiency as well as road types and slopes. For these various reasons, drivers may take different routes on different occasions. Second, while the exact path choice of followers among many possible choices remains ambiguous, we consider the worst-case in terms of the damage costs to the leader and formulate pessimistic bilevel optimization problems. This is in accordance with the current practices in installations of WIM stations, which are typically located in the most damaged road links (Martin et al., 2014; Reagor, 2002).

Accordingly, we present two pessimistic formulations. In the first pessimistic formulation, we consider the maximum degree of ambiguity in the route choice of unlawful travelers. While the first pessimistic formulation yields the most robust design of facility locations, the attitude can be overly pessimistic. To overcome this limitation, we provide the second pessimistic formulation, which can flexibly control the level of pessimism on the behavior of unlawful travelers between optimistic and overly pessimistic assumptions. Resulting pessimistic formulations yield trilevel optimization problems (Sinha et al., 2018). Consequently, a single-level reduction, widely used in optimistic formulations of bilevel optimization problems, where the objectives of a leader and follower collide, is not obtainable for pessimistic formulations in general. Because of such structural differences, solution methods designed for optimistic formulations are not directly applicable for solving pessimistic formulations (Wiesemann et al., 2013; Zare et al., 2018). Therefore, in addition to formulating the general case of the EFCP, we present a cutting plane algorithm to solve the pessimistic formulation exactly.

A recent study by Arslan et al. (2018) has expedited solution times of the EFCP by using a path-cut formulation that enumerates unintercepted paths on the fly. The path-cut based method, however, is only applicable to the optimistic formulation with a specific cost function. In this paper, we consider generic cost functions in deriving exact solutions for the pessimistic formulations. In particular, we construct cost functions not only looking at the lengths of links, but also taking into account critical infrastructure elements such as bridges, tunnels and etc.

The main contributions of this study are as follows. To the best of our knowledge, this study is the first to present the EFCP considering the bounded rationality of drivers and general cost structures, for which no algorithm is available. Within the proposed framework, two pessimistic formulations of the problem are presented, which yield a robust network design and allow control over the level of pessimism on the behaviors of drivers. The proposed cutting-plane algorithm solves the pessimistic EFCP exactly and generalizes to various forms of cost functions. As our numerical studies on real networks suggest, the pessimistic formulations prevent up to 13.25% more damage

to the network compared to optimistic formulations, highlighting the vulnerability of optimizing behavior assumptions.

The remainder of the paper will proceed as follows. In Section 2, we state the problem formally and discuss the properties of the commonly used assumption in the literature and the resulting formulations. By relaxing assumptions on the travelers' behavior, we present two pessimistic bilevel formulations in Sections 3 and 4. In Section 5, we discuss solution methods. In Section 6, we demonstrate the numerical study results. Lastly, in Section 7, we give concluding remarks.

2 The Evasive Flow Capturing Problem

In a given network $\mathcal{G}(\mathcal{N}, \mathcal{A})$, with a set of nodes $\mathcal{N}$ and a set of arcs $\mathcal{A}$, let us consider a set of vehicle flows, $\mathcal{F}$. Each flow $f \in \mathcal{F}$ is characterized by an origin-destination pair and a deviation tolerance factor $\lambda_f > 0$. $\xi_{s_f t_f}$ represents the length of the shortest path between origin node s_f and destination node t_f for flow f.

Definition 1 (Acceptable Path). A path is called *acceptable* for flow f, if its length is at most $\bar{\lambda}_f$, where $\bar{\lambda}_f = \lambda_f \xi_{s_f t_f}$.

Definition 2 (Unintercepted Path). A path is called *unintercepted* for flow f, if it enables traversing without passing any law enforcement facilities. Accordingly, flow f is intercepted if it does not possess an unintercepted path.

Then for each flow $f \in \mathcal{F}$, $\bar{\lambda}_f$ induces a restricted set of nodes $\mathcal{N}_f \subset \mathcal{N}$ and a restricted set of arcs $\mathcal{A}_f \in \mathcal{A}$. For each arc $(i,j) \in \mathcal{A}_f$ we have $\xi_{s_f i} + d_{ij} + \xi_{jt_f} \leq \bar{\lambda}_f$, where d_{ij} is the length of arc (i,j), s_f is origin node and t_f is destination node for flow f. Then $\mathcal{N}_f$ represents all nodes in $\mathcal{A}_f$, which is the same as the notion of non-dominated arcs and nodes in Arslan et al. (2018).

The EFCP naturally fits the bilevel setting, where the government (the leader) decides the location of law enforcement facilities and unlawful travelers (followers) aim to drive on unintercepted acceptable paths. Then the set of leader's feasible decisions can be defined as follows:

$$\mathbf{X} = \big\{ \mathbf{x} : x_{ij} \in \{0,1\} \quad \forall (i,j) \in \mathcal{A} \big\}. \tag{1}$$

where x_{ij} is a binary variable, whose value equals 1 if a law enforcement facility is located on arc (i,j) and 0 otherwise. Accordingly, vector $\mathbf{x}$ represents all x_{ij} variables for all $(i,j) \in \mathcal{A}$. We define the set of feasible reactions of followers for any given leader's decision $\mathbf{x} \in \mathbf{X}$:

$$\mathbf{L}^f(\mathbf{x}) = \left\{ (\mathbf{r}^f, u_f) \left| \begin{array}{ll} \displaystyle\sum_{(i,j)\in\mathcal{A}_f} r_{ij}^f - \sum_{(j,i)\in\mathcal{A}_f} r_{ji}^f = \begin{cases} u_f & \text{if } i = s_f \\ -u_f & \text{if } i = t_f \quad \forall i \in \mathcal{N}_f, \\ 0 & \text{otherwise} \end{cases} \\ r_{ij}^f \leq 1 - x_{ij} & \forall (i,j) \in \mathcal{A}_f, \\ u_f, r_{ij}^f \in \{0,1\} & \forall (i,j) \in \mathcal{A}_f \end{array} \right. \right\} \tag{2}$$

4

where u_f is a binary variable whose value is equal to 1 if flow f is unintercepted and 0 otherwise. Another binary variable r_{ij}^f indicates if arc (i,j) is selected for the follower's path or not. Then vector $\mathbf{r}^f$ represents all r_{ij}^f variables for all $(i,j) \in \mathcal{A}_f$.

We define the set of best responses of followers (Arslan et al., 2018):

$$\mathbb{L}_0^f(\mathbf{x}) = \operatorname*{arg\,max}_{(\mathbf{r}^f, u_f) \in \mathbf{L}^f(\mathbf{x})} \left\{ (\bar{\lambda}_f + \delta)u_f - \sum_{(i,j) \in \mathcal{A}_f} d_{ij} r_{ij}^f \right\} \tag{3}$$

Note that δ is a sufficiently small positive constant so that the addition of δ has no impact on comparing the path length. In practice, δ can be smaller than the data precision. In the above problem, if the length of the shortest unintercepted path exceeds $\bar{\lambda}_f$, then u_f becomes 0; so does $\mathbf{r}^f$. Therefore, the optimal objective function value of the lower-level problem is always nonnegative; hence, $\sum_{(i,j) \in \mathcal{A}_f} d_{ij} r_{ij}^f \leq \bar{\lambda}_f$. We use $\mathbf{L}(\mathbf{x})$ to denote the Cartesian product $\prod_{f \in \mathcal{F}} \mathbf{L}^f(\mathbf{x}) = \mathbf{L}^1(\mathbf{x}) \times \mathbf{L}^2(\mathbf{x}) \times \cdots \times \mathbf{L}^{|\mathcal{F}|}(\mathbf{x})$. Similarly, $\mathbb{L}_0(\mathbf{x}) = \prod_{f \in \mathcal{F}} \mathbb{L}_0^f(\mathbf{x})$.

Arslan et al. (2018) proposed the following evasive flow capturing problem as a bilevel optimization problem, where the leader aims to minimize installation costs and damage to network induced by followers:

$$\mathbf{BM}: \quad \underset{\mathbf{x}, \mathbf{r}, \mathbf{u}}{\text{minimize}} \quad \left[\sum_{(i,j) \in \mathcal{A}} w_{ij} x_{ij} + \sum_{f \in \mathcal{F}} \sum_{(i,j) \in \mathcal{A}_f} h_{ij}^f r_{ij}^f \right] \tag{4}$$

$$\text{subject to} \quad \mathbf{x} \in \mathbf{X} \tag{5}$$

$$(\mathbf{r}, \mathbf{u}) \in \mathbb{L}_0(\mathbf{x}) \tag{6}$$

where w_{ij} is cost of installation at arc (i,j) and h_{ij}^f is cost of damage to arc (i,j) caused by flow f. Arslan et al. (2018) deployed a specific damage cost function, namely $h_{ij}^f = c^f d_{ij}$ with constant cost coefficient c^f for flow f and relied on the following assumptions:

Assumption 1. Arslan et al. (2018) assumed the following behavior of the followers (unlawful travelers):

(a) The followers drive on the shortest unintercepted acceptable path.

(b) If no unintercepted acceptable path is available, then a follower does not travel.

Figure 1 illustrates the above assumptions, where black nodes denote intercepted paths and white nodes denote unintercepted paths. Then according to Assumption 1, followers select the shortest unintercepted path.

The bilevel formulation **BM** can be reformulated as a single-level optimization problem by replacing the lower-level problem by a set of optimality conditions. Using the duality and bounding some dual variables by $\bar{\lambda}_f + \delta$, a single-level formulation without big-M has been proposed in Arslan et al. (2018).
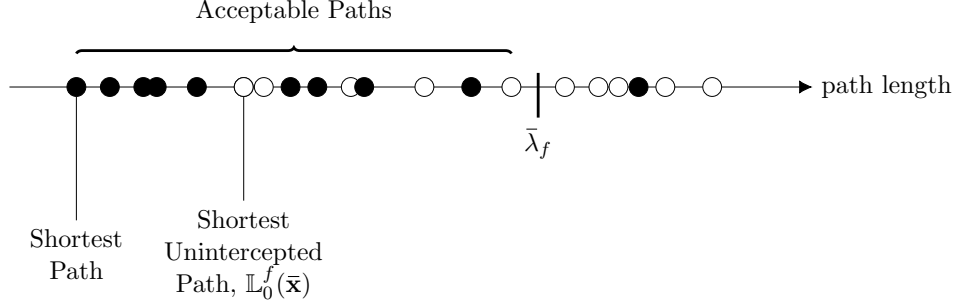
Figure 1: Followers take the unintercepted shortest path in Assumption 1. (●: intercepted path, ○: unintercepted path)

However, Arslan et al. (2018) shows the superiority of the following path-cut formulation compared to the obtained single-level formulation.

$$\mathbf{PM}: \quad \underset{\mathbf{x},\mathbf{r},\mathbf{u}}{\text{minimize}} \quad \left[\sum_{(i,j)\in\mathcal{A}} w_{ij}x_{ij} + \sum_{f\in\mathcal{F}}\sum_{(i,j)\in\mathcal{A}_f} h_{ij}^f r_{ij}^f \right] \tag{7}$$

$$\text{subject to} \quad 1 - \sum_{(i,j)\in\mathcal{A}^p} x_{ij} \leq u_f \qquad \forall f \in \mathcal{F}, p \in \mathcal{P}^f \tag{8}$$

$$\mathbf{x} \in \mathbf{X} \tag{9}$$

$$(\mathbf{r},\mathbf{u}) \in \mathbf{L}(\mathbf{x}) \tag{10}$$

Note that $\mathcal{P}^f$ is the set of all acceptable paths and $\mathcal{A}^p$ is the set of arcs in path p. Although the number of constraints (8) is exponential, by adding them as lazy constraints with other heuristic cuts, we do not need to enumerate all acceptable paths *a priori*; instead, the next shortest unintercepted acceptable path will be generated and a constraint will be added on the fly.

While the performance of **PM** has been demonstrated to exceed the performance of the single-level model of Marković et al. (2015), it has some limitations in a few manners. We note that **PM** does not enforce Assumption 1(a) explicitly, while Assumption 1(b) has been considered in the definition of $\mathcal{P}^f$. By considering $h_{ij}^f = c^f d_{ij}$ in the objective function, **PM** automatically selects the *shortest* unintercepted acceptable path for each $f \in \mathcal{F}$. The competitive performance of **PM** can therefore be explained, because the number of lazy constraints to be generated is expected to be small with the objectives of the leader and the follower being the same.

As pointed out by Hooshmand and MirHassani (2018), the condition $h_{ij}^f = c^f d_{ij}$ is not necessarily observed in practice. However, for networks with $h_{ij}^f \neq c^f d_{ij}$, **PM** will assume that the followers will choose the *least harmful* path among all unintercepted acceptable paths. Therefore, in general settings, **PM** is no longer equivalent to **BM**.

Note that the **BM** formulation in the previous section is called an *optimistic* formulation, regardless of whether $h_{ij}^f = c^f d_{ij}$ or not. That is, when there are multiple optimal solutions in the lower level, the leader assumes that the followers will cooperatively choose the least harmful choice. On the other hand, when the followers are assumed to be non-cooperative, thus they select

the most harmful paths, we can write the *vanilla* pessimistic formulation as follows:

$$\mathbf{PeBM_0}: \quad \underset{\mathbf{x}\in\mathbf{X}}{\text{minimize}} \left[\sum_{(i,j)\in\mathcal{A}} w_{ij}x_{ij} + \max_{(\mathbf{r},\mathbf{u})\in\mathbb{L}_0(\mathbf{x})} \sum_{f\in\mathcal{F}} \sum_{(i,j)\in\mathcal{A}_f} h_{ij}^f r_{ij}^f \right], \tag{11}$$

which we call $\mathbf{PeBM_0}$. Note that the bilevel nature is embedded in the definition of the set $\mathbb{L}_0(\mathbf{x})$ as the lower-level problem, while the upper-level problem is a minimax optimization problem. To contrast the above pessimistic formulation with the original optimistic formulation $\mathbf{BM}$, we may write $\mathbf{BM}$ as follows:

$$\mathbf{BM}: \quad \underset{\mathbf{x}\in\mathbf{X}}{\text{minimize}} \left[\sum_{(i,j)\in\mathcal{A}} w_{ij}x_{ij} + \min_{(\mathbf{r},\mathbf{u})\in\mathbb{L}_0(\mathbf{x})} \sum_{f\in\mathcal{F}} \sum_{(i,j)\in\mathcal{A}_f} h_{ij}^f r_{ij}^f \right]. \tag{12}$$

In practical applications, $\mathbf{PeBM_0}$ unlikely makes a meaningful contribution, since in many practical networks, the shortest unintercepted path is usually unique, i.e. $\mathbb{L}_0(\mathbf{x})$ is a singleton for most $\mathbf{x}$, especially when link travel cost d_{ij} is not integer valued. Therefore, the vanilla pessimistic formulation $\mathbf{PeBM_0}$ is not the topic of this study. Indeed, we consider non-optimizing followers with ambiguous preferences and present pessimistic formulations accordingly.

3   The Pessimistic Formulation

Even though the assumption of optimizing the behavior of travelers prevails in modeling followers' reactions in the existing literature, it does not always hold, mainly for the following two reasons. First, followers may not always select the shortest path. Instead of choosing the shortest path, followers may accept a reasonably short path, especially when travel time along paths is uncertain. Second, the leader, or the modeler, cannot observe the exact cost coefficient in the followers' optimization problem. Hence, the exact choice of followers remains ambiguous. To consider such ambiguity, we relax Assumptions 1(a) and model ambiguous path choices as follows:

Assumption 2 (PeBM). We assume the following behavior of the followers (unlawful travelers):

(a) The followers drive on an unintercepted acceptable path, but the exact path choice is ambiguous.

(b) If no unintercepted acceptable path is available, then the follower does not travel.

Figure 2 illustrates the new assumption, where black circles represent intercepted paths and white circles represent unintercepted paths. Then according to Assumption 2, followers may select any unintercepted path whose length is less than or equal to the threshold $\bar{\lambda}_f$ for each flow $f \in \mathcal{F}$.

To present a bilevel pessimistic formulation under Assumption 2, we perturb the cost function of follower $f \in \mathcal{F}$ by vector $\boldsymbol{\sigma}^f = (\sigma_{ij}^f : (i,j) \in \mathcal{A}_f)$. For any given perturbation vector $\boldsymbol{\sigma}^f$, we
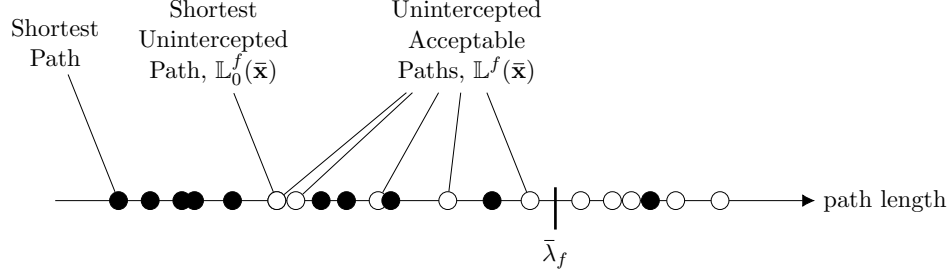
Figure 2: The path choice of followers is ambiguous among unintercepted acceptable paths in Assumption 2. (●: intercepted path, ○: unintercepted path)

Table 1: List of formulations and symbols related to the followers' responses

Symbol	Description
BM	the optimistic formulation as in Assumption 1
PeBM$_0$	the vanilla pessimistic formulation as in Assumption 1
PeBM	the pessimistic formulation as in Assumption 2
PeBM$_\epsilon$	the pessimistic formulation as in Assumption 3
L	the set of feasible solutions of followers; see (2)
Given leader's decision $\mathbf{x}$:	
$\mathbb{L}_0(\mathbf{x})$	the set of unambiguous responses of followers as in Assumption 1; see (3)
$\mathbb{L}(\mathbf{x})$	the set of *ambiguous* responses of followers as in Assumption 2; see (14)
$\mathbb{L}_\epsilon(\mathbf{x})$	the set of *ambiguous* responses of followers as in Assumption 3, given satisficing threshold ϵ; see (17)
Given leader's decision $\mathbf{x}$ and perturbation $\boldsymbol{\sigma}$:	
$\mathfrak{L}(\mathbf{x};\boldsymbol{\sigma})$	the set of followers' perturbed responses used inside $\mathbb{L}(\mathbf{x})$; see (13)
$\mathfrak{L}_\epsilon(\mathbf{x};-\boldsymbol{\sigma})$	the set of followers' perturbed responses used inside $\mathbb{L}_\epsilon(\mathbf{x})$, given satisficing threshold ϵ; see (16)

define the set of optimal responses of follower $f \in \mathcal{F}$:

$$\mathfrak{L}^f(\mathbf{x};\boldsymbol{\sigma}^f) = \underset{(\mathbf{r}^f,u_f)\in\mathbf{L}^f(\mathbf{x})}{\arg\max} \left\{ (\bar{\lambda}_f + \delta)u_f - \sum_{(i,j)\in\mathcal{A}_f} (d_{ij} + \sigma_{ij}^f)r_{ij}^f \right\}. \tag{13}$$

Note that $\mathbb{L}_0^f(\mathbf{x}) = \mathfrak{L}^f(\mathbf{x};\mathbf{0})$. For a bounded set of perturbation vectors

$$\boldsymbol{\Sigma}^f = \left\{ \boldsymbol{\sigma}^f : 0 \le \sigma_{ij}^f \le \bar{\lambda}_f + \delta \quad \forall (i,j) \in \mathcal{A}_f \right\},$$

we also define the set of ambiguous responses of follower $f \in \mathcal{F}$:

$$\mathbb{L}^f(\mathbf{x}) = \left\{ (\mathbf{r}^f, u_f) \in \mathfrak{L}^f(\mathbf{x};\boldsymbol{\sigma}^f) : \boldsymbol{\sigma}^f \in \boldsymbol{\Sigma}^f \right\}. \tag{14}$$

We let $\boldsymbol{\Sigma} = \prod_{f\in\mathcal{F}} \boldsymbol{\Sigma}^f$ and $\mathbb{L}(\mathbf{x}) = \prod_{f\in\mathcal{F}} \mathbb{L}^f(\mathbf{x})$. We use a few different symbols related to the followers' responses. We summarize them in Table 1 for the convenience of readers.

We show that $\mathbb{L}(\mathbf{x})$ leads to an equivalent set of followers' responses as described in Assumption

8

2. First, we show that any element of $\mathbb{L}(\mathbf{x})$ is an unintercepted acceptable path; hence satisfies the conditions in Assumption 2.

Proposition 1. *For any given $\mathbf{x} \in \mathbf{X}$, we let $(\widehat{\mathbf{r}}^f, \widehat{u}_f) \in \mathbb{L}^f(\mathbf{x})$ for each $f \in \mathcal{F}$. Then, we have $\sum_{(i,j) \in \mathcal{A}_f} d_{ij} \widehat{r}^f_{ij} \leq \bar{\lambda}_f$ for all $f \in \mathcal{F}$.*

We also show that the converse is true; that is, any possible response from Assumption 2 is an element of $\mathbb{L}^f(\mathbf{x})$. We first consider an unintercepted acceptable path and then show that it can be an optimal solution to (13) for a particular perturbation vector $\widehat{\boldsymbol{\sigma}}^f \in \boldsymbol{\Sigma}^f$.

Proposition 2. *Consider any upper-level solution $\bar{\mathbf{x}}$. For each $f \in \mathcal{F}$, let $(\widehat{\mathbf{r}}^f, \widehat{u}_f) \in \mathbf{L}^f(\bar{\mathbf{x}})$ such that $\sum_{(i,j) \in \mathcal{A}_f} d_{ij} \widehat{r}^f_{ij} \leq \bar{\lambda}_f$. Define $\widehat{\boldsymbol{\sigma}}^f \in \boldsymbol{\Sigma}^f$ such that*

$$
\widehat{\sigma}^f_{ij} = \begin{cases} \bar{\lambda}_f + \delta & \text{if } \widehat{r}^f_{ij} = 0 \\ 0 & \text{if } \widehat{r}^f_{ij} = 1 \end{cases}.
\tag{15}
$$

Then $(\widehat{\mathbf{r}}^f, \widehat{u}_f) \in \mathfrak{L}^f(\mathbf{x}; \widehat{\boldsymbol{\sigma}}^f)$ and, consequently, $(\widehat{\mathbf{r}}^f, \widehat{u}_f) \in \mathbb{L}^f(\bar{\mathbf{x}})$.

Propositions 1 and 2 indicate the equivalency between $\mathbb{L}^f(\mathbf{x})$ and Assumption 2. Using this equivalency, we present a bilevel pessimistic formulation as follows:

$$
\textbf{PeBM}: \quad \underset{\mathbf{x} \in \mathbf{X}}{\text{minimize}} \left[\sum_{(i,j) \in \mathcal{A}} w_{ij} x_{ij} + \max_{(\mathbf{r}, \mathbf{u}) \in \mathbb{L}(\mathbf{x})} \sum_{f \in \mathcal{F}} \sum_{(i,j) \in \mathcal{A}_f} h^f_{ij} r^f_{ij} \right].
$$

Note that $\mathbb{L}_0(\mathbf{x})$ is a subset of $\mathbb{L}(\mathbf{x})$. Therefore, **PeBM** considers more pessimistic behavior of followers or yields a more robust solution to the leader, than **PeBM$_0$**. As defined earlier in (13) and (14), set $\mathbb{L}(\mathbf{x})$ consists of optimal solutions to optimization problems. Therefore, **PeBM** involves tri-level optimization problems. We devise an exact algorithm for solving **PeBM** in Section 5.

4   The ϵ-Pessimistic Formulation

In Assumption 1, followers are assumed always to take the unintercepted *shortest* path, leading to an optimistic formulation in **BM**. On the other hand, since Assumption 2 considers ambiguity among all unintercepted *acceptable* paths, the modeling of followers can be overly pessimistic with **PeBM**. In this section, we develop a formulation that can flexibly control the level of pessimism on the behavior of followers between optimistic and overly pessimistic.

Figure 3 demonstrates the key idea. While there are five unintercepted acceptable paths available, we assume that followers will only choose the first three paths, since the lengths of those three paths are 'short enough' within a certain threshold. The first three paths are called *satisficing* paths, which are formally defined as follows:

Definition 3 (Satisficing Path). For each follower $f \in \mathcal{F}$, a path is called *satisficing* with threshold $\epsilon_f > 0$, if its length is shorter than $(1 + \epsilon_f)\xi_f$, where ξ_f is the length of the shortest unintercepted path between s_f and t_f.
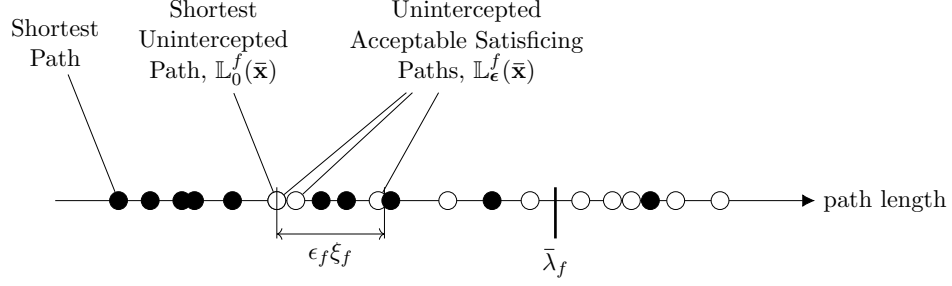
Figure 3: The path choice of followers is ambiguous among unintercepted acceptable satisficing paths in Assumption 3. (●: intercepted path, ○: unintercepted path)

Note that as the facility location decision in the upper-level changes, the unintercepted shortest path may change and correspondingly the set of satisficing paths may also change. Some satisficing paths are also *subpath*-satisficing, as defined by Sun et al. (2018):

Definition 4 (Subpath-Satisficing Path)**.** For each follower $f \in \mathcal{F}$, a path is called *subpath-satisficing* with threshold $\epsilon_f > 0$, if any subpath, including itself, is a satisficing path with the same threshold ϵ_f.

We limit our interest to subpath-satisficing paths, for a reason to be clearer later in Proposition 4. In this section, we make the following assumption:

Assumption 3 (PeBM$_\epsilon$). We assume the following behavior of the followers (unlawful travelers):

(a) The followers drive on an unintercepted acceptable path, but the exact path choice is ambiguous among subpath-satisficing paths.

(b) If no unintercepted acceptable path is available, then the follower does not travel.

To provide a formulation that is consistent with Assumption 3, we introduce new variables and sets. Let $\bar{\boldsymbol{\lambda}} = (\bar{\lambda}_f : f \in \mathcal{F})$ and $\boldsymbol{\epsilon} = (\epsilon_f : f \in \mathcal{F})$. For any $\boldsymbol{\epsilon} \geq \mathbf{0}$, we define

$$\mathcal{L}_{\boldsymbol{\epsilon}}^f(\mathbf{x}; -\boldsymbol{\sigma}^f) = \underset{(\mathbf{r}^f, u_f) \in \mathbf{L}^f(\mathbf{x})}{\arg\max} \left\{ \frac{\bar{\lambda}_f + \delta}{1 + \epsilon_f} u_f - \sum_{(i,j) \in \mathcal{A}_f} (d_{ij} - \sigma_{ij}^f) r_{ij}^f \right\}. \tag{16}$$

We define new sets of perturbation vectors:

$$\boldsymbol{\Sigma}_{\boldsymbol{\epsilon}}^f = \left\{ \boldsymbol{\sigma}^f : 0 \leq \sigma_{ij}^f \leq \frac{\epsilon_f}{1 + \epsilon_f} d_{ij} \quad \forall (i,j) \in \mathcal{A}_f \right\}$$

and $\boldsymbol{\Sigma}_{\boldsymbol{\epsilon}} = \prod_{f \in \mathcal{F}} \boldsymbol{\Sigma}_{\boldsymbol{\epsilon}}^f$. We also define

$$\mathbb{L}_{\boldsymbol{\epsilon}}^f(\mathbf{x}) = \left\{ (\mathbf{r}^f, u_f) \in \mathcal{L}_{\boldsymbol{\epsilon}}^f(\mathbf{x}; -\boldsymbol{\sigma}^f) : \boldsymbol{\sigma}^f \in \boldsymbol{\Sigma}_{\boldsymbol{\epsilon}}^f \right\} \tag{17}$$

10

and $\mathbb{L}_{\epsilon}(\mathbf{x}) = \prod_{f \in \mathcal{F}} \mathbb{L}_{\epsilon}^f(\mathbf{x})$. Refer to Table 1 for various symbols used for modeling followers' decision problems.

With the new set $\mathbb{L}_{\epsilon}(\mathbf{x})$, we present a bilevel pessimistic formulation as follows:

$$\mathbf{PeBM}_{\epsilon}: \quad \underset{\mathbf{x}}{\text{minimize}} \quad \left[\sum_{(i,j) \in \mathcal{A}} w_{ij} x_{ij} + \max_{(\mathbf{r},\mathbf{u}) \in \mathbb{L}_{\epsilon}(\mathbf{x})} \sum_{f \in \mathcal{F}} \sum_{(i,j) \in \mathcal{A}_f} h_{ij}^f r_{ij}^f \right]$$

$$\text{subject to} \quad x_{ij} \in \{0,1\} \qquad\qquad\qquad \forall (i,j) \in \mathcal{A}.$$

We prove that $\mathbf{PeBM}_{\epsilon}$ is indeed consistent with Assumption 3. First, we consider any element of $\mathbb{L}_{\epsilon}(\mathbf{x})$ and show that it corresponds to an unintercepted subpath-satisficing, acceptable path.

Proposition 3. *For each $f \in \mathcal{F}$, given $\mathbf{x} \in \mathbf{X}$, let $(\mathring{\mathbf{r}}^f, \mathring{u}_f) \in \mathbb{L}_0^f(\mathbf{x})$ and let $(\widehat{\mathbf{r}}^f, \widehat{u}_f) \in \mathbb{L}_{\epsilon}^f(\mathbf{x})$. Then the following conditions hold:*

$$\sum_{(i,j) \in \mathcal{A}_f} d_{ij} \widehat{r}_{ij}^f \leq \bar{\lambda}_f, \tag{18}$$

$$\sum_{(i,j) \in \mathcal{A}_f} d_{ij} \widehat{r}_{ij}^f \leq (1 + \epsilon_f) \sum_{(i,j) \in \mathcal{A}_f} d_{ij} \mathring{r}_{ij}^f, \tag{19}$$

for all $f \in \mathcal{F}$.

We now consider the converse. Unfortunately, the converse does not hold exactly. That is, a satisficing path is not necessarily an optimal solution to the follower's problem. Instead, only a subset of satisficing paths correspond to optimal solutions to the lower-level problem; in particular, the set of subpath-satisficing paths.

The following result is immediate from Sun et al. (2018, Theorem 6):

Proposition 4. *For each $f \in \mathcal{F}$, given $\mathbf{x} \in \mathbf{X}$, let $(\mathring{\mathbf{r}}^f, \mathring{u}_f) \in \mathbb{L}_0^f(\mathbf{x})$. Consider any subpath-satisficing path represented by $(\widehat{\mathbf{r}}^f, \widehat{u}_f) \in \mathbf{L}^f(\mathbf{x})$ with $\widehat{u}_f = 1$. That is, $\sum_{(i,j) \in \mathcal{A}_f} d_{ij} \widehat{r}_{ij}^f \leq (1 + \epsilon_f) \bar{\lambda}_f$ and $\sum_{(i,j) \in \mathcal{A}_f} d_{ij} \widehat{r}_{ij}^f \leq (1 + \epsilon_f) \sum_{(i,j) \in \mathcal{A}_f} d_{ij} \mathring{r}_{ij}^f$. Then $(\widehat{\mathbf{r}}^f, \widehat{u}_f) \in \mathbb{L}_{\epsilon}^f(\mathbf{x})$, in particular for the following $\widehat{\sigma}_{ij}^f$:*

$$\widehat{\sigma}_{ij}^f = \frac{\epsilon_f}{1 + \epsilon_f} d_{ij} \widehat{r}_{ij}^f = \begin{cases} \dfrac{\epsilon_f}{1 + \epsilon_f} d_{ij} & \text{if } \widehat{r}_{ij}^f = 1 \\ 0 & \text{if } \widehat{r}_{ij}^f = 0 \end{cases} \tag{20}$$

for all $(i,j) \in \mathcal{A}_f$.

The results in Propositions 3 and 4 indicate that $\mathbf{PeBM}_{\epsilon}$ is closely related to the ϵ-approximation to the general pessimistic bilevel optimization problem in the literature (Wiesemann et al., 2013). In particular, defining a shorthand for the objective function of followers $f \in \mathcal{F}$:

$$g_f(\mathbf{r}^f, u_f) = (\bar{\lambda}_f + \delta) u_f - \sum_{(i,j) \in \mathcal{A}_f} d_{ij} r_{ij}^f,$$

11

we may write the ϵ-approximation as follows:

$$\underset{\mathbf{x}\in\mathbf{X}}{\text{minimize}} \quad \left[\sum_{(i,j)\in\mathcal{A}} w_{ij}x_{ij} + \max_{(\mathbf{r},\mathbf{u})\in\widetilde{\mathbb{L}}_{\epsilon}(\mathbf{x})} \sum_{f\in\mathcal{F}}\sum_{(i,j)\in\mathcal{A}_f} h_{ij}^f r_{ij}^f\right],$$

where

$$\widetilde{\mathbb{L}}_{\epsilon}^f(\mathbf{x}) = \left\{(\bar{\mathbf{r}}^f, \bar{u}_f) \in \mathbf{L}^f(\mathbf{x}) : g_f(\bar{\mathbf{r}}^f, \bar{u}_f) > g_f(\mathbf{r}^f, u_f) - \epsilon_f \quad \forall(\mathbf{r}^f, u_f) \in \mathbf{L}^f(\mathbf{x})\right\},$$

for any $\epsilon > \mathbf{0}$. In Propositions 3 and 4, we have shown that our definition of $\mathbb{L}_{\epsilon}^f(\mathbf{x})$ leads to the following relationship:

$$\mathbb{L}_{\epsilon}^f(\mathbf{x}) = \left\{(\bar{\mathbf{r}}^f, \bar{u}_f) \in \mathfrak{L}_{\epsilon}^f(\mathbf{x}; \boldsymbol{\sigma}) : \boldsymbol{\sigma}^f \in \boldsymbol{\Sigma}_{\epsilon}^f\right\}$$

$$\subseteq \left\{(\bar{\mathbf{r}}^f, \bar{u}_f) \in \mathbf{L}^f(\mathbf{x}) : g_f(\bar{\mathbf{r}}^f, \bar{u}_f) \geq \frac{1}{1+\epsilon_f} g_f(\mathbf{r}^f, u_f) \quad \forall(\mathbf{r}^f, u_f) \in \mathbf{L}^f(\mathbf{x})\right\},$$

for any $\epsilon \geq \mathbf{0}$. The last 'subset' relation is due to the subpath-satisficing path consideration as in Proposition 4. While ϵ in $\widetilde{\mathbb{L}}_{\epsilon}^f(\mathbf{x})$ is additive, ϵ in $\mathbb{L}_{\epsilon}^f(\mathbf{x})$ is multiplicative.

Note that $\mathbb{L}_0^f(\mathbf{x})$ given in (3) can be restated as follows:

$$\mathbb{L}_0^f(\mathbf{x}) = \underset{(\mathbf{r}^f, u_f)\in\mathbf{L}^f(\mathbf{x})}{\arg\max} \; g_f(\mathbf{r}^f, u_f)$$

$$\equiv \left\{(\bar{\mathbf{r}}^f, \bar{u}_f) \in \mathbf{L}^f(\mathbf{x}) : g_f(\bar{\mathbf{r}}^f, \bar{u}_f) \geq g_f(\mathbf{r}^f, u_f) \quad \forall(\mathbf{r}^f, u_f) \in \mathbf{L}^f(\mathbf{x})\right\}.$$

While both $\widetilde{\mathbb{L}}_{\epsilon}(\mathbf{x})$ and $\mathbb{L}_{\epsilon}(\mathbf{x})$ approach to $\mathbb{L}_0(\mathbf{x})$ as $\epsilon \to \mathbf{0}$, we see that $\widetilde{\mathbb{L}}_{\epsilon}(\mathbf{x})$ is not defined at $\epsilon = \mathbf{0}$. Apparently, $\mathbb{L}_{\epsilon}(\mathbf{x}) \equiv \mathbb{L}_0(\mathbf{x})$ when $\epsilon = \mathbf{0}$. In general, we have the following relationship for any given $\mathbf{x} \in \mathbf{X}$: $\mathbb{L}_{\mathbf{0}}(\mathbf{x}) \subseteq \mathbb{L}_{\epsilon}(\mathbf{x}) \subseteq \mathbb{L}(\mathbf{x})$ for any $\epsilon \geq \mathbf{0}$.

5   Solution Methods

The discussed pessimistic formulations result in trilevel optimization problems. Namely, the master problem based on the decision of the leader is followed by the worst-case problem (WCP) of the follower. The latter problem itself has a bilevel structure, where a follower selects the most damaging route among unintercepted paths with length at most λ. We first present the cutting plane algorithm to solve the **PeBM** and then introduce the single-level reformulation of the WCP. Later, we introduce similar techniques to solve the **PeBM**$_\epsilon$ formulation.

5.1   The Cutting Plane Algorithm

We propose a cutting plane algorithm to solve the problem **PeBM**. Consider the following master problem, which is a relaxation of **PeBM**:

$$\textbf{Master}: \quad \underset{\mathbf{x},\mathbf{r},\mathbf{u}}{\text{minimize}} \quad \left[\sum_{(i,j)\in\mathcal{A}} w_{ij}x_{ij} + \sum_{f\in\mathcal{F}}\sum_{(i,j)\in\mathcal{A}_f} h_{ij}^f r_{ij}^f \right] \tag{21}$$

$$\text{subject to} \quad \mathbf{x} \in \mathbf{X} \tag{22}$$

$$(\mathbf{r},\mathbf{u}) \in \mathbf{L}(\mathbf{x}) \tag{23}$$

$$\{\text{cuts are added iteratively}\}.$$

Let $\bar{\mathbf{x}}$ and $\bar{\mathbf{r}}^f$ denote an optimal solution to the master problem.

Given the master solution, we solve the following worst-case problem (WCP) to generate feasible reactions of followers:

$$\textbf{WCP}(\bar{\mathbf{x}}): \quad \underset{\mathbf{r},\mathbf{u}}{\text{maximize}} \quad \sum_{f\in\mathcal{F}}\sum_{(i,j)\in\mathcal{A}_f} h_{ij}^f r_{ij}^f \tag{24}$$

$$\text{subject to} \quad (\mathbf{r},\mathbf{u}) \in \mathbb{L}(\bar{\mathbf{x}}) \tag{25}$$

Let a solution of the worst-case problem be $\widehat{\mathbf{r}}^f$ and $\widehat{u}_f$ for each $f \in \mathcal{F}$.

Given the two pairs of solutions, we add cuts. For each $f \in \mathcal{F}$, we compare the paths chosen by $\bar{\mathbf{r}}^f$ and $\widehat{\mathbf{r}}^f$. We focus on the distinct subpaths, which are definite as not identical arcs in $\bar{\mathbf{r}}^f$ and $\widehat{\mathbf{r}}^f$, and denote them as $\bar{p}$ and $\widehat{p}$ respectively. We add the following cuts motivated by Gzara (2013) and Liu and Kwon (2020) for each $f \in \mathcal{F}$ adjusting them to the possibility of followers not traveling:

- If $\bar{u}_f{=}1$ and $\widehat{u}_f{=}1$, we add the following cut:

$$\sum_{(i,j)\in\widehat{p}} x_{ij} \geq 1 - |\bar{p}| + \sum_{(i,j)\in\bar{p}} r_{ij}^f. \tag{26}$$

- If $\bar{u}_f{=}0$ and $\widehat{u}_f{=}1$, we add the following cut:

$$\sum_{(i,j)\in\widehat{p}} x_{ij} \geq 1 - u_f. \tag{27}$$

- If $\bar{u}_f{=}0$ and $\widehat{u}_f{=}0$, we add no additional cut.

Cut (26) indicates that at least one arc in subpath $\widehat{p}$ must be intercepted to reroute flow f to subpath $\bar{p}$. The form of cut (26) is first proposed by Gzara (2013) and later simplified by Liu and Kwon (2020). In the second case when the travel demand varies in the two solutions, we add a new type of cut (27), which indicates that at least one arc in subpath $\widehat{p}$ must be intercepted in order to disable traversing of flow f. The case with $\bar{u}_f = 1$ and $\widehat{u}_f = 0$ should not occur by the
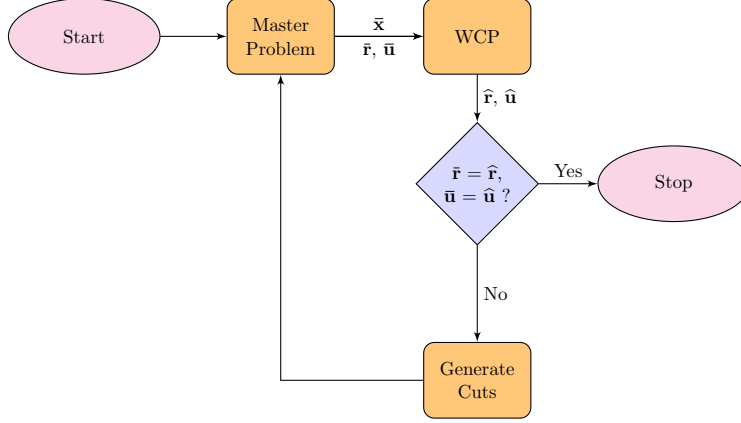
Figure 4: The overview of the cutting plane algorithm

nature of the worst-case problem. Note that cuts (26) and (27) do not require creating any new variables; therefore they can potentially be used as lazy constraints. We repeat this procedure until the master solution and the worst-case solution coincide, i.e. $\bar{\mathbf{x}} = \hat{\mathbf{x}}$. Thus, when dual bound of **PeBM** (represented by the solution of the master problem) and its upper bound (represented by the WCP solution) match, the cutting plane algorithm terminates.

We show that cuts (26) and (27) do not cut out the optimal solution $(\mathbf{x}^*, \mathbf{r}^*, \mathbf{u}^*)$.

Proposition 5. *Suppose* **WCP**$(\mathbf{x})$ *has the unique optimal solution for any given* $\mathbf{x} \in \mathbf{X}$. *Then, any optimal solution of* **PeBM** *is feasible to* **Master**.

Although it is unlikely in realistic cases, there could exist multiple optimal solutions to **WCP**$(\bar{\mathbf{x}})$ and, therefore, multiple optimal solutions to **PeBM**. In such cases, the cutting plane algorithm may cut out an optimal solution, but it assures that at least one optimal solution is feasible to the master problem.

Due to the structural similarity between **PeBM**$_\epsilon$ and **PeBM**, we can apply the same cutting plane algorithm for the latter formulation. The master problem is the same as given in (21)–(23) and the cut generation procedure is the same as well. The structure of the worst-case problem is also the same, although we need to replace $\mathbb{L}(\cdot)$ by $\mathbb{L}_\epsilon(\cdot)$. That is, For **PeBM**$_\epsilon$, we solve the following worst-case problem (WCP), given the master solution:

$$\mathbf{WCP}_\epsilon(\bar{\mathbf{x}}): \quad \underset{\mathbf{r}, \mathbf{u}}{\text{maximize}} \quad \sum_{f \in \mathcal{F}} \sum_{(i,j) \in \mathcal{A}_f} h_{ij}^f r_{ij}^f \tag{28}$$

$$\text{subject to} \quad (\mathbf{r}, \mathbf{u}) \in \mathbb{L}_\epsilon(\bar{\mathbf{x}}) \tag{29}$$

We let the solution of the worst-case problem be $\hat{\mathbf{r}}^f$ and $\hat{u}_f$ for each $f \in \mathcal{F}$. Overall, Figure 4 summarizes the cutting plane algorithm for both formulations.

5.2 Single Level Reformulation of WCP($\bar{\mathbf{x}}$)

While the proposed cutting plane algorithm can be combined with any solution method for the WCP, we can reduce the trilevel structure of the pessimistic formulations by reformulating the underlying WCP.

Note that the worst-case problem in (24)–(25) itself is a bilevel optimization problem of the following form:

$$\underset{\boldsymbol{\sigma}^f}{\text{maximize}} \quad \sum_{(i,j)\in\mathcal{A}_f} h_{ij}^f r_{ij}^f \tag{30}$$

$$\text{subject to} \quad \boldsymbol{\sigma}^f \in \boldsymbol{\Sigma}^f \tag{31}$$

$$\underset{\mathbf{r}^f, u_f}{\text{maximize}} \quad (\bar{\lambda}_f + \delta)u_f - \sum_{(i,j)\in\mathcal{A}_f} (d_{ij} + \sigma_{ij}^f)r_{ij}^f \tag{32}$$

$$\text{subject to} \quad \sum_{(i,j)\in\mathcal{A}_f} r_{ij}^f - \sum_{(j,i)\in\mathcal{A}_f} r_{ji}^f = \begin{cases} u_f & \text{if } i = s_f \\ -u_f & \text{if } i = t_f \\ 0 & \text{otherwise} \end{cases} \quad \forall i \in \mathcal{N}_f, \tag{33}$$

$$r_{ij}^f \leq 1 - \bar{x}_{ij} \qquad \forall(i,j) \in \mathcal{A}_f, \tag{34}$$

$$u_f, r_{ij}^f \in \{0, 1\} \qquad \forall(i,j) \in \mathcal{A}_f \tag{35}$$

for each $f \in \mathcal{F}$. Using Propositions 1 and 2, we can easily show the following statement holds.

Corollary 1. *Suppose that* $(\bar{\mathbf{r}}, \bar{\mathbf{u}}, \bar{\boldsymbol{\sigma}})$ *is an optimal solution to* (30)–(35). *Define* $\widehat{\boldsymbol{\sigma}}^f \in \boldsymbol{\Sigma}^f$ *such that*

$$\widehat{\sigma}_{ij}^f = \begin{cases} \bar{\lambda}_f + \delta & \text{if } \bar{r}_{ij}^f = 0 \\ 0 & \text{if } \bar{r}_{ij}^f = 1 \end{cases} \tag{36}$$

for all $f \in \mathcal{F}$. *Then* $(\bar{\mathbf{r}}, \bar{\mathbf{u}}, \widehat{\boldsymbol{\sigma}})$ *is also an optimal solution to* (30)–(35).

Using Corollary 1, we can simplify the presentation of (30)–(35) via a change of variables and derive an equivalent single-level reformulation to (30)–(35).

Proposition 6. *Any optimal solution to the following single-level optimization problem is also an optimal solution to the worst-case problem* **WCP**($\bar{\mathbf{x}}$) *in* (24)–(25):

$$\underset{\mathbf{r}^f, u_f, \boldsymbol{\pi}^f, \boldsymbol{\mu}^f}{\text{maximize}} \quad \sum_{(i,j)\in\mathcal{A}_f} h_{ij}^f r_{ij}^f \tag{37}$$

$$\text{subject to} \quad \sum_{(i,j)\in\mathcal{A}_f} r_{ij}^f - \sum_{(j,i)\in\mathcal{A}_f} r_{ji}^f \leq \begin{cases} u_f & \text{if } i = s_f \\ -u_f & \text{if } i = t_f \\ 0 & \text{otherwise} \end{cases} \quad \forall i \in \mathcal{N}_f, \tag{38}$$

$$r_{ij}^f \leq 1 - \bar{x}_{ij} \qquad \forall(i,j) \in \mathcal{A}_f, \tag{39}$$

15

$$\pi_j^f \leq \pi_i^f + d_{ij} + (\bar{\lambda}_f + \delta)(\bar{x}_{ij}^f + 1 - r_{ij}^f) \qquad\qquad (i,j) \in \mathcal{A}_f \qquad\qquad (40)$$

$$(\bar{\lambda}_f + \delta)(1 - u_f) + \sum_{(i,j) \in \mathcal{A}_f} d_{ij} r_{ij}^f \leq \pi_{t_f}^f - \pi_{s_f}^f \qquad\qquad (41)$$

$$(\bar{\lambda}_f + \delta)u_f - \sum_{(i,j) \in \mathcal{A}_f} d_{ij} r_{ij}^f \geq 0 \qquad\qquad (42)$$

$$r_{ij}^f, u_f \in \{0,1\} \qquad\qquad \forall (i,j) \in \mathcal{A}_f \qquad\qquad (43)$$

$$\pi_i^f, \mu_{ij}^f \geq 0 \qquad\qquad \forall i \in \mathcal{N}_f, (i,j) \in \mathcal{A}_f \qquad (44)$$

for each $f \in \mathcal{F}$.

The dual variable π_i^f can be interpreted as a label for an unintercepted path with length at most $\bar{\lambda}_f$ from s_f to node i and $\pi_{t_f}^f - \pi_{s_f}^f$ represents the length of the chosen path. We can provide useful insights regarding the properties of the WCP. Constraint (41) serves as a switch for u_f to determine whether flow f is on or off and constraint (42) ensures that the path length does not exceed the threshold. Constraint (40), obtained from the dual feasibility condition, serves as a sub-tour elimination constraint essentially, where a dual variable π_i^f can be interpreted as a label for the chosen path with length at most $\bar{\lambda}_f$ from s_f to node i. The form of constraint (40) is popularly used in the literature of vehicle routing problems with time windows for tracking the arrival time of each vehicle in each node (Erdoğan and Miller-Hooks, 2012; Schneider et al., 2014). The subtour elimination constraint (40) is particularly useful for the worst-case problem, since the problem is a maximization problem. Note also that one can remove links $(i,j) \in \mathcal{A}_f$ such that $\bar{x}_{ij} = 1$ and corresponding constraints (39) and (40) from the problem to reduce the problem size, since $\bar{\mathbf{x}}$ is not a variable for this worst-case problem.

When $u_f = 1$, the worst-case problem is indeed an instance of the Elementary Shortest Path Problem with Resource Constraints (ESPPRC). In fact, the resource constraint is induced by the lengths of an unintercepted acceptable path given the solution of the master problem and reduced cost is represented by cost of damage to the network. ESPPRC typically arises in solving vehicle routing problems and exact algorithms have been proposed for solving the problem using cycle elimination techniques (Irnich and Villeneuve, 2006). Lozano et al. (2015) develop a pulse algorithm based on implicit enumeration of paths with novel bounding techniques to prune paths. Instead of using the single-level reformulation (SLR) given in (37)–(44), we can use the pulse algorithm of Lozano et al. (2015) as follows. First, for given $\bar{\mathbf{x}}$, remove links $(i,j) \in \mathcal{A}_f$ such that $\bar{x}_{ij} = 1$. Then, find the unintercepted shortest path for each $f \in \mathcal{F}$. If the length of the unintercepted shortest path exceeds $\bar{\lambda}_f$, then set $u_f = 0$. If not, find the most harmful unintercepted acceptable path using the pulse algorithm by redefining the reduced cost as the cost of damage and set $\mathbf{r}^f$ accordingly.

5.3 Single Level Reformulation of $\mathbf{WCP}_{\boldsymbol{\epsilon}}(\bar{\mathbf{x}})$

The $\mathbf{WCP}_{\boldsymbol{\epsilon}}(\bar{\mathbf{x}})$ can be restated as follows:

$$\underset{\boldsymbol{\sigma}^f}{\text{maximize}} \quad \sum_{(i,j)\in\mathcal{A}_f} h_{ij}^f r_{ij}^f \tag{45}$$

$$\text{subject to} \quad 0 \leq \sigma_{ij}^f \leq \frac{\epsilon_f}{1+\epsilon_f} d_{ij} \qquad \forall(i,j)\in\mathcal{A}_f \tag{46}$$

$$\underset{\mathbf{r}^f, u_f}{\text{maximize}} \quad \frac{\bar{\lambda}_f + \delta}{1+\epsilon_f} u_f - \sum_{(i,j)\in\mathcal{A}_f} (d_{ij} - \sigma_{ij}^f) r_{ij}^f \tag{47}$$

$$\text{subject to} \quad \sum_{(i,j)\in\mathcal{A}_f} r_{ij}^f - \sum_{(j,i)\in\mathcal{A}_f} r_{ji}^f \leq \begin{cases} u_f & \text{if } i = s_f \\ -u_f & \text{if } i = t_f \\ 0 & \text{otherwise} \end{cases} \qquad \forall i \in \mathcal{N}_f, \tag{48}$$

$$\bar{x}_{ij} r_{ij}^f \leq 0 \qquad \forall(i,j)\in\mathcal{A}_f, \tag{49}$$

$$u_f, r_{ij}^f \in \{0,1\} \qquad \forall(i,j)\in\mathcal{A}_f \tag{50}$$

for each $f \in \mathcal{F}$.

Proposition 7. *Any optimal solution to the following single-level optimization problem is also an optimal solution to the worst-case problem* $\mathbf{WCP}_{\boldsymbol{\epsilon}}(\bar{\mathbf{x}})$ *in* (28)–(29):

$$\underset{\mathbf{r}^f, u_f, \boldsymbol{\sigma}^f}{\text{maximize}} \quad \sum_{(i,j)\in\mathcal{A}_f} h_{ij}^f r_{ij}^f \tag{51}$$

$$\text{subject to} \quad \sum_{(i,j)\in\mathcal{A}_f} r_{ij}^f - \sum_{(j,i)\in\mathcal{A}_f} r_{ji}^f \leq \begin{cases} u_f & \text{if } i = s_f \\ -u_f & \text{if } i = t_f \\ 0 & \text{otherwise} \end{cases} \qquad \forall i \in \mathcal{N}_f, \tag{52}$$

$$r_{ij}^f \leq 1 - \bar{x}_{ij} \qquad \forall(i,j)\in\mathcal{A}_f, \tag{53}$$

$$\pi_j^f \leq \pi_i^f + d_{ij} - \frac{\epsilon_f}{1+\epsilon_f} d_{ij} r_{ij}^f + (\bar{\lambda}_f + \delta)\bar{x}_{ij} \qquad \forall(i,j)\in\mathcal{A}_f \tag{54}$$

$$\frac{\bar{\lambda}_f + \delta}{1+\epsilon_f}(1 - u_f) + \sum_{(i,j)\in\mathcal{A}_f} d_{ij} r_{ij}^f - \frac{\epsilon_f}{1+\epsilon_f} \sum_{(i,j)\in\mathcal{A}_f} d_{ij} r_{ij}^f \leq \pi_{t_f}^f - \pi_{s_f}^f \tag{55}$$

$$\frac{\bar{\lambda}_f + \delta}{1+\epsilon_f} u_f - \sum_{(i,j)\in\mathcal{A}_f} d_{ij} r_{ij}^f + \frac{\epsilon_f}{1+\epsilon_f} \sum_{(i,j)\in\mathcal{A}_f} d_{ij} r_{ij}^f \geq 0 \tag{56}$$

$$u_f, r_{ij}^f \in \{0,1\} \qquad \forall(i,j)\in\mathcal{A}_f \tag{57}$$

$$\pi_k^f, u^f \geq 0 \qquad \forall k \in \mathcal{N}_f \tag{58}$$

for each $f \in \mathcal{F}$.

Again instead of using the single-level reformulation (SLR) for $\mathbf{WCP}_{\boldsymbol{\epsilon}}(\bar{\mathbf{x}})$, we can use the

following procedure. First, for given $\bar{\mathbf{x}}$, remove links $(i, j) \in \mathcal{A}_f$ such that $\bar{x}_{ij} = 1$. Then, find the length of the unintercepted shortest path for each $f \in \mathcal{F}$, denoted by ξ_f. If the length of the unintercepted shortest path exceeds $\bar{\lambda}_f$, then set $u_f = 0$. If not, find the most harmful unintercepted path with length at most $(1 + \epsilon_f)\xi_f$ by using the pulse algorithm for the ESPPRC. However, as discussed in Section 4, not all satisfying paths are subpath satisfying paths. Therefore, for any given path with the length at most $(1 + \epsilon_f)\xi_f$, we need to check if it is a subpath satisfying path using techniques discussed in Sun et al. (2018). Then we can set $\mathbf{r}^f$ accordingly.

6   Numerical Experiments

In this section, we present the experimental setup and used network data to evaluate the performance of the cutting plane algorithm for **PeBM** and **PeBM$_\epsilon$**. We implement algorithms using Julia programming language under Windows and CPLEX 12.8.0 and use a computer with Intel Core i7-4790 3.60-GHz processors with 16 GB RAM. A machine has 8 cores and each experiment was run using up to 8 threads. To solve the underlying problem in both formulations of the WCP, the elementary shortest path with resource constraint algorithm by Lozano et al. (2015) is implemented. We use the LightGraphs library for graphical computations including Dijkstra's algorithm (see Bromberger et al. (2017) for full documentation).

6.1   Data Description

For the numerical studies, we use several datasets. The first dataset is the 25-node network used by Arslan et al. (2018). The second group of datasets is generated randomly. We place randomly the different numbers of nodes (we use 30, 50, 70 and 100 nodes) on a 100 miles by 100 miles grid and randomly connect arcs, so that the density of the network is equal to ρ and arcs' lengths are defined in the euclidean distance. We consider two values of ρ equal to either 0.2 or 0.4, which is defined as the ratio of the number of arcs to the number of arcs in a complete graph with the same number of nodes. We generate a different number of origin-destination pairs, where the distance between origin and destination nodes is at least 60 miles. We also assign randomly a number of flows in links ranging from 20 to 8000.

As a test on a real network, we employ the Albany network data used in hazardous materials transportation (Kang et al., 2014b,a). The data represents the transportation network around the Albany county, NY consisting of seven interstate and US highways. Damage to a link is calculated as the product of the number of flows passing and the probability of link damage, which itself accounts for the population density and link length (details can be found in Kang et al. (2014b)). We generate random origin-destination pairs whose distance is at least 17.5 miles (the average shortest distance among all nodes in the network).

We use realistic values of WIM installation costs defined in thousands of dollars presented in Marković et al. (2015). For followers cost of damage, similar to Hooshmand and MirHassani (2018), we consider cost coefficient $c_{ij} = \$4/\text{mile}$ for all $(i, j) \in \mathcal{A}$. Vulnerability coefficients μ_{ij} are

Table 2: Performance of the cutting plane algorithm for PeBM

| | $\lambda_f = 1.0$ | | | | $\lambda_f = 1.5$ | | | | $\lambda_f = 2.0$ | | | |
| | CPUTime, sec | | Iter | | CPUTime, sec | | Iter | | CPUTime, sec | | Iter | |
$w_{ij}, \$$	Pulse	SLR	Pulse	SLR	Pulse	SLR	Pulse	SLR	Pulse	SLR	Pulse	SLR
10k	13.30	6.38	2.60	2.60	15.33	14.31	3.20	3.20	26.81	59.35	5.00	5.20
60k	13.31	6.68	2.80	2.80	15.64	15.02	3.20	3.40	30.55	60.88	5.60	5.60
110k	13.37	6.93	2.80	3.00	16.36	17.79	4.80	4.80	28.63	62.62	6.20	6.20
160k	13.33	6.95	2.80	3.00	13.77	17.26	4.80	4.80	30.55	68.25	7.00	7.20
260k	13.44	7.20	3.00	3.20	17.05	20.98	6.40	6.40	39.42	75.46	8.80	8.40
360k	13.55	7.81	4.00	3.60	17.10	22.71	7.20	7.20	55.20	89.05	10.40	10.00

Table 3: Performance of the cutting plane algorithm for PeBM$_\epsilon$

| | $\lambda_f = 1.0$ | | | | $\lambda_f = 1.5$ | | | | $\lambda_f = 2.0$ | | | |
| | CPUTime, sec | | Iter | | CPUTime, sec | | Iter | | CPUTime, sec | | Iter | |
$w_{ij}, \$$	Pulse	SLR	Pulse	SLR	Pulse	SLR	Pulse	SLR	Pulse	SLR	Pulse	SLR
10k	15.56	6.48	2.60	2.60	15.55	9.14	2.80	2.80	18.60	12.15	2.80	3.00
60k	12.95	6.25	2.80	2.80	18.63	10.71	3.20	3.20	19.53	14.00	3.60	3.60
110k	15.76	7.06	3.00	3.00	18.99	11.45	3.60	3.60	16.17	12.55	3.40	3.40
160k	15.78	7.06	3.00	3.00	19.20	12.53	4.20	4.20	19.73	15.75	4.40	4.40
260k	15.96	7.32	3.20	3.20	19.58	14.14	4.80	5.00	21.96	20.48	6.20	5.80
360k	16.12	7.85	3.60	3.60	16.92	13.39	5.00	5.00	20.80	22.47	6.40	6.40

introduced to account for various vulnerable structures such as bridges and tunnels. Then the total damage cost to arc from flow $\mathcal{F}$ is computed as follows: $h_{ij}^f = c_{ij} d_{ij} \mu_{ij} n_f$, where n_f is a number of vehicles in flow $\mathcal{F}$ and μ_{ij} is randomly drawn from $\{1.0, 1.5, 2.0\}$ for each $(i, j) \in \mathcal{A}$. The value of δ is set to 0.1, 0.1, and 0.01 for the 25-node network, random networks, and the Albany network, respectively.

6.2 The 25-node network

Table 2 shows the performance of the cutting plane algorithm for the **PeBM** formulation using the 25-node network. With varying values of λ, we measure (with five replicates) the computational time and a number of iterations of the algorithm when we solve the WCP either by the pulse algorithm presented in Lozano et al. (2015) or using the single-level reformulation obtained in Section 5. In general, applying the pulse algorithm expedites the solution. The computational time difference of both methods is evident with a large value of λ and installation cost. Solving the SLR optimization problem becomes harder as the number of ambiguous paths increases with λ and installation costs become more comparable to the damage costs of followers. Similarly, Table 3 presents the cutting plane algorithm performance in solving the **PeBM$_\epsilon$** formulation. In this case, we observe that the single level reformulation of the WCP with satisfying paths performs better than the pulse algorithm in terms of the computational time. In general, the number of iterations of the SLR is comparable to the number of iterations under the pulse algorithm.

To assess the value of pessimistic formulations we introduce a new term called the value of pessimistic solutions, VPS. Let $\mathbf{x}^{BM}$, $\mathbf{x}^{PeBM}$, and $\mathbf{x}^{PeBM_\epsilon}$ be an optimal solution of **BM**, **PeBM**,

Table 4: The value of the pessimistic formulation, PeBM

	Total Costs			Installation Costs		Cost of Damage	
$w_{ij}, \$$	Opt.	Pess.	VPS, %	Opt.	Pess.	Opt.	Pess.
10k	426,787	426,787	0.00	420,000	420,000	6,787	6,787
60k	2,492,636	2,492,636	0.00	2,328,000	2,328,000	164,636	164,636
110k	4,389,244	4,387,012	0.05	4,048,000	4,070,000	341,244	317,012
160k	6,258,940	6,184,900	1.12	5,536,000	5,568,000	722,940	616,900
260k	9,759,323	9,420,499	3.42	7,904,000	8,216,000	1,855,323	1,204,499
360k	13,471,236	12,525,926	6.86	9,648,000	11,088,000	3,823,236	1,437,926

and $\mathbf{PeBM}_\epsilon$, respectively. We write the upper-level objective functions of $\mathbf{PeBM}$

$$Z(\mathbf{x}) = \sum_{(i,j)\in\mathcal{A}} w_{ij}x_{ij} + \max_{(\mathbf{r},\mathbf{u})\in\mathbb{L}(\mathbf{x})} \sum_{f\in\mathcal{F}} \sum_{(i,j)\in\mathcal{A}_f} h_{ij}^f r_{ij}^f$$

and that of $\mathbf{PeBM}_\epsilon$

$$Z_\epsilon(\mathbf{x}) = \sum_{(i,j)\in\mathcal{A}} w_{ij}x_{ij} + \max_{(\mathbf{r},\mathbf{u})\in\mathbb{L}_\epsilon(\mathbf{x})} \sum_{f\in\mathcal{F}} \sum_{(i,j)\in\mathcal{A}_f} h_{ij}^f r_{ij}^f$$

Then, the VPS for $\mathbf{PeBM}$ can be defined as follows:

$$\text{VPS} = \frac{Z(\mathbf{x}^{\text{BM}}) - Z(\mathbf{x}^{\text{PeBM}})}{Z(\mathbf{x}^{\text{BM}})} \tag{59}$$

Similarly, the VPS for $\mathbf{PeBM}_\epsilon$ can be defined as follows:

$$\text{VPS} = \frac{Z_\epsilon(\mathbf{x}^{\text{BM}}) - Z_\epsilon(\mathbf{x}^{\text{PeBM}_\epsilon})}{Z_\epsilon(\mathbf{x}^{\text{BM}})}. \tag{60}$$

We run experiments measuring the total costs under the solutions of optimistic and pessimistic formulations of the EFCP. We implement the optimistic formulation presented in (12) and again use the pulse algorithm to solve the underlying elementary shortest path problem with the resource constraint. Table 4 illustrates that the value of the VPS for $\mathbf{PeBM}$ may reach up to 6.86% depending on installation costs. However, damage costs caused by unlawful travelers under the optimistic solutions may exceed damage costs under the pessimistic solutions of the $\mathbf{PeBM}$ more than two times as shown in Table 4 with $w_{ij} = \$360k$. In general, pessimistic solutions require to install more WIM stations, thus requiring a higher initial investment, which can be justified by the preventable damage costs compared to the optimistic solutions. In the case of $\mathbf{PeBM}_\epsilon$ as shown in Table 5, solutions of the optimistic and pessimistic solutions are similar in most cases when we let the value of $\epsilon_f = 70\%$. However, with increased installation costs we observe similar results as in the case of $\mathbf{PeBM}$.

Table 5: The value of the pessimistic formulation, PeBM$_\epsilon$, $\epsilon = 70\%$

w_{ij}, \$	Total Costs			Installation Costs		Cost of Damage	
	Opt.	Pess.	VPS, %	Opt.	Pess.	Opt.	Pess.
10k	426,302	426,302	0.00	420,000	420,000	6,302	6,302
60k	2,492,913	2,492,913	0.00	2,328,000	2,328,000	164,913	164,913
110k	4,368,018	4,368,018	0.00	4,048,000	4,048,000	320,018	320,018
160k	6,198,784	6,144,769	0.83	5,536,000	5,568,000	662,784	576,769
260k	9,519,564	9,419,416	1.05	8,008,000	8,216,000	1,511,564	1,203,416
360k	12,506,229	12,417,145	0.71	9,864,000	10,224,000	2,642,229	2,193,145

Table 6: Random network results for PeBM

			$w_{ij} =$ \$110k						$w_{ij} =$ \$160k					
Network			CPUTime, sec		Iter		Gap, %		CPUTime, sec		Iter		Gap, %	
$\mathcal{N}$	ρ	$\mathcal{F}$	Pulse	SLR	Pulse	SLR	Pulse	SLR	Pulse	SLR	Pulse	SLR	Pulse	SLR
30	0.2	20	2.68	1.41	7.6	7.8	0	0	2.72	1.61	9.6	9.6	0	0
		50	2.74	2.45	7.2	7.4	0	0	2.71	2.37	7.2	7.2	0	0
	0.4	20	2.97	2.88	17.4	17.0	0	0	3.92	7.85	32.2	31.4	0	0
		50	3.03	4.17	12.0	11.4	0	0	0.49	3.74	13.0	11.8	0	0
50	0.2	20	2.99	3.04	19.4	18.8	0	0	3.02	3.06	19.0	18.8	0	0
		50	3.65	6.01	17.6	16.6	0	0	4.59	9.11	24.0	23.6	0	0
	0.4	20	2.95	2.97	18.2	17.4	0	0	2.98	3.02	17.2	18.2	0	0
		50	4.10	9.38	28.0	25.0	0	0	4.38	10.09	26.0	26.2	0	0
70	0.2	20	4.57	8.36	39.8	43.6	0	0	14.69	21.36	57.8	56.6	0	0
		50	3.79	7.59	18.6	19.2	0	0	4.76	8.03	19.8	19.2	0	0
	0.4	20	6.49	15.74	72.4	73.4	0	0	12.59	21.05	68.6	69.0	0	0
		50	258.85	333.10	206.8	206.4	0	0	170.02	225.41	137.6	142.6	0	0
100	0.2	20	8.84	28.80	4.86	29.40	0	0	6.93	27.60	5.26	27.60	0	0
		50	5.71	26.20	13.99	28.20	0	0	9.63	27.40	17.27	27.20	0	0
100	0.4	20	2288.91	301.00	2519.20	309.00	0	0	39631.85	497.00	38264.41	542.00	13.61	14.94
		50	47897.73	205.00	48772.74	198.00	27.07	22.82	55651.64	120.00	54974.55	130.00	37.09	30.99

Table 7: Random network results for PeBM$_\epsilon$ with $\epsilon_f \in [15\%, 20\%]$

			$w_{ij} =$ \$110k				$w_{ij} =$ \$160k			
Network			CPUTime, sec		Iter		CPUTime, sec		Iter	
$\mathcal{N}$	ρ	$\mathcal{F}$	Pulse	SLR	Pulse	SLR	Pulse	SLR	Pulse	SLR
30	0.2	20	3.03	1.26	6.4	6.4	3.06	1.42	8.0	8.0
		50	3.16	1.90	5.2	5.4	3.18	1.93	5.6	5.6
	0.4	20	3.49	1.87	10.0	10.2	3.47	1.85	9.2	9.8
		50	3.92	3.01	9.0	8.4	3.93	3.06	8.2	8.6
50	0.2	20	5.09	5.15	26.6	26.4	3.30	1.83	9.4	10.2
		50	4.97	5.09	14.0	13.0	4.27	4.23	13.8	12.4
	0.4	20	7.99	9.24	42.2	42.4	3.72	2.28	12.2	13.0
		50	14.58	19.62	27.8	29.2	5.57	7.04	22.2	19.8
70	0.2	20	5.09	5.15	26.6	26.4	10.29	12.73	38.0	40.6
		50	4.97	5.09	14.0	13.0	5.25	5.52	13.6	13.6
	0.4	20	7.99	9.24	42.2	42.4	10.05	10.98	42.8	41.6
		50	14.58	19.62	27.8	29.2	14.64	19.16	28.8	28.4
100	0.2	20	4.88	3.86	19.8	19.6	2.45	4.19	20.4	20.8
		50	7.06	9.34	18.2	18.8	7.73	10.22	20.2	20.4
	0.4	20	133.13	148.10	122.0	121.6	133.13	148.10	122.0	121.6
		50	12123.16	12460.66	313.0	310.6	12123.16	12460.66	313.0	310.6

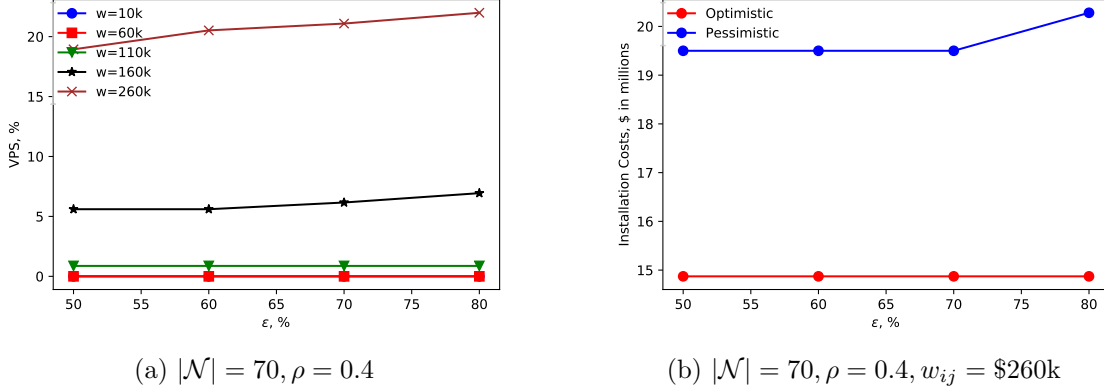(a) $|\mathcal{N}| = 70, \rho = 0.4$ (b) $|\mathcal{N}| = 70, \rho = 0.4, w_{ij} = \$260k$

Figure 5: Results for the random networks using the **PeBM$_\epsilon$** formulation

6.3 The random networks

In order to further evaluate the performance of the cutting plane algorithm for both formulations, we test them on randomly generated networks of different sizes and a number of flows (with 5 replications of each setting). Tables 6 and 7 demonstrate the performance of the proposed cutting plane for the PeBM and PeBM$_\epsilon$ formulations respectively, where $\lambda_f = 2$. The experiments results suggest the efficient performance of the algorithm for the most of instances for the PeBM formulation, while the instance with 100 nodes and $\rho = 0.4$ is not solved within an hour time limit with the gaps reported in the table. The reason for such performance can be explained by a large number of nodes, strong connectivity within the network and a large value of λ. In the case of the PeBM$_\epsilon$, where ϵ values are drawn randomly between 15% and 20%, all instances are solved in a reasonable amount of time, including the instance with 100 nodes and $\rho = 0.4$.

To measure the gains associated with the pessimistic solutions, we again measure the value of VPS on the random networks. Table 8 shows the VPS values with varying values of installation costs for random networks. In general, as installation costs increase the value of VPS increases. Also, as shown in Figure 5a the value of the VPS increases with the increased value of ϵ. We also have to note that under the optimistic solution, installation costs remain the same with the increased value of ϵ, while under the pessimistic solution the installation costs increase as shown in Figure 5b.

6.4 The Albany network

To assess the value of pessimistic solutions on the real network, we conduct experiments measuring the VPS values. As shown in Figure 6a, the value of VPS on the Albany network can reach up to 13.25% for $w_{ij} = \$260k$ and 12.97% for $w_{ij} = \$360k$ even for small values of ϵ, highlighting the benefits of the pessimistic solutions. We also observe constant VPS values with the increased value of ϵ for $w_{ij} = \$260k$, which is due to the nature of damage cost to the network. In particular, since for the Albany network, the damage costs of followers is estimated not only considering the lengths

Table 8: The value of pessimistic solutions for PeBM$_\epsilon$, random networks, $\rho = 0.4$

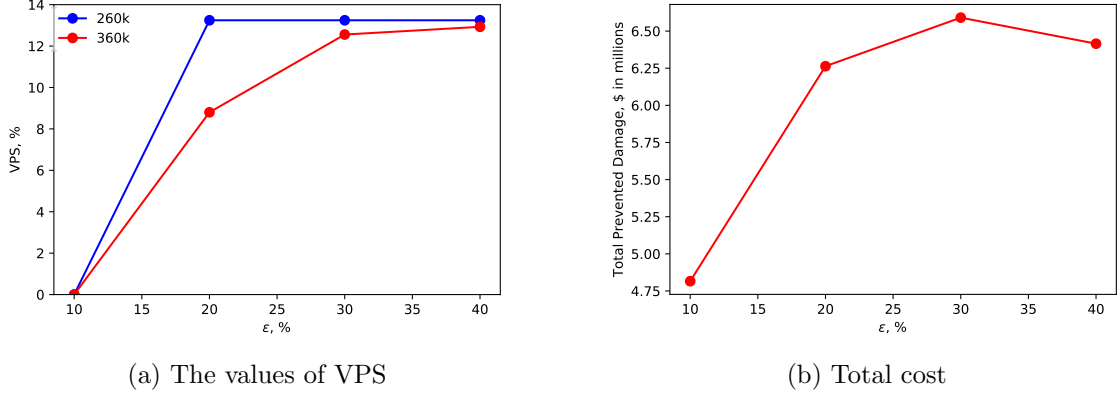| ϵ	$|\mathcal{N}|$	w_{ij}, \$	Total Costs		VPS, %	Installation Costs		Damage	
			Opt.	Pess.		Opt.	Pess.	Opt.	Pess.
0.5	30	10	360,000	360,000	0.00	360,000	360,000	0	0
		60	2,700,000	2,700,000	0.00	2,700,000	2,700,000	0	0
		110	4,213,420	3,932,688	6.53	3,520,000	3,762,000	693,420	170,688
		160	5,831,220	5,585,824	4.19	4,960,000	5,216,000	871,220	369,824
		260	8,931,220	8,756,512	1.94	8,060,000	8,216,000	871,220	540,512
	50	10	450,000	450,000	0.00	450,000	450,000	0	0
		60	2,700,000	2,700,000	0.00	2,700,000	2,700,000	0	0
		110	4,950,000	4,950,000	0.00	4,950,000	4,950,000	0	0
		160	7,200,000	7,200,000	0.00	7,200,000	7,200,000	0	0
		260	11,897,088	11,640,864	2.14	10,400,000	11,284,000	1,497,088	356,864
	70	10	830,000	830,000	0.00	830,000	830,000	0	0
		60	4,980,000	4,980,000	0.00	4,980,000	4,980,000	0	0
		110	9,213,352	9,130,000	0.87	9,064,000	9,130,000	149,352	0
		160	14,070,504	13,268,872	5.60	12,128,000	13,088,000	1,942,504	180,872
		260	26,190,384	21,197,760	18.94	14,872,000	19,500,000	11,318,384	1,697,760
0.6	30	10	360,000	360,000	0.00	360,000	360,000	0	0
		60	2,160,000	2,160,000	0.00	2,160,000	2,160,000	0	0
		110	4,373,440	3,960,000	9.22	3,520,000	3,960,000	853,440	0
		160	5,991,240	5,760,000	3.84	4,960,000	5,760,000	1,031,240	0
		260	9,091,240	9,031,664	0.65	8,060,000	8,164,000	1,031,240	867,664
	50	10	450,000	450,000	0.00	450,000	450,000	0	0
		60	2,700,000	2,700,000	0.00	2,700,000	2,700,000	0	0
		110	4,950,000	4,950,000	0.00	4,950,000	4,950,000	0	0
		160	7,200,000	7,200,000	0.00	7,200,000	7,200,000	0	0
		260	11,897,088	11,640,864	2.14	10,400,000	11,284,000	1,497,088	356,864
	70	10	830,000	830,000	0.00	830,000	830,000	0	0
		60	4,980,000	4,980,000	0.00	4,980,000	4,980,000	0	0
		110	9,213,352	9,130,000	0.87	9,064,000	9,130,000	149,352	0
		160	14,070,504	13,268,872	5.60	12,128,000	13,088,000	1,942,504	180,872
		260	26,721,188	21,197,760	20.52	14,872,000	19,500,000	11,849,188	1,697,760
0.7	30	10	360,000	360,000	0.00	360,000	360,000	0	0
		60	2,160,000	2,160,000	0.00	2,160,000	2,160,000	0	0
		110	4,380,552	3,960,000	9.36	3,520,000	3,960,000	860,552	0
		160	6,019,688	5,760,000	4.30	4,960,000	5,760,000	1,059,688	0
		260	9,119,688	9,101,908	0.20	8,060,000	8,060,000	1,059,688	1,041,908
	50	10	450,000	450,000	0.00	450,000	450,000	0	0
		60	2,700,000	2,700,000	0.00	2,700,000	2,700,000	0	0
		110	4,950,000	4,950,000	0.00	4,950,000	4,950,000	0	0
		160	7,200,000	7,200,000	0.00	7,200,000	7,200,000	0	0
		260	12,271,360	11,700,000	4.63	10,400,000	11,700,000	1,871,360	0
	70	10	830,000	830,000	0.00	830,000	830,000	0	0
		60	4,980,000	4,980,000	0.00	4,980,000	4,980,000	0	0
		110	9,213,352	9,130,000	0.87	9,064,000	9,130,000	149,352	0
		160	14,160,940	13,280,000	6.16	12,128,000	13,280,000	2,032,940	0
		260	27,143,116	21,382,564	21.09	14,872,000	19,500,000	12,271,116	1,882,564
0.8	30	10	360,000	360,000	0.00	360,000	360,000	0	0
		60	2,160,000	2,160,000	0.00	2,160,000	2,160,000	0	0
		110	4,448,116	3,960,000	10.64	3,520,000	3,960,000	928,116	0
		160	6,087,252	5,760,000	5.34	4,960,000	5,760,000	1,127,252	0
		260	9,187,252	9,169,472	0.20	8,060,000	8,060,000	1,127,252	1,109,472
	50	10	450,000	450,000	0.00	450,000	450,000	0	0
		60	2,700,000	2,700,000	0.00	2,700,000	2,700,000	0	0
		110	4,950,000	4,950,000	0.00	4,950,000	4,950,000	0	0
		160	7,200,000	7,200,000	0.00	7,200,000	7,200,000	0	0
		260	12,375,808	11,700,000	5.46	10,400,000	11,700,000	1,975,808	0
	70	10	830,000	830,000	0.00	830,000	830,000	0	0
		60	4,980,000	4,980,000	0.00	4,980,000	4,980,000	0	0
		110	9,213,352	9,130,000	0.87	9,064,000	9,130,000	149,352	0
		160	14,282,796	13,280,000	6.94	12,128,000	13,280,000	2,154,796	0
		260	27,534,888	21,467,004	21.99	14,872,000	20,280,000	12,662,888	1,187,004

(a) The values of VPS

(b) Total cost

Figure 6: The Albany network results for the **PeBM$_\epsilon$** formulation $\lambda = 1.2$

Table 9: Location of WIM systems with constraints on the installation budget and the number of installations on Albany network, $\epsilon = 20\%$. Distinct locations between the optimistic and pessimistic solutions are shown in bold face.
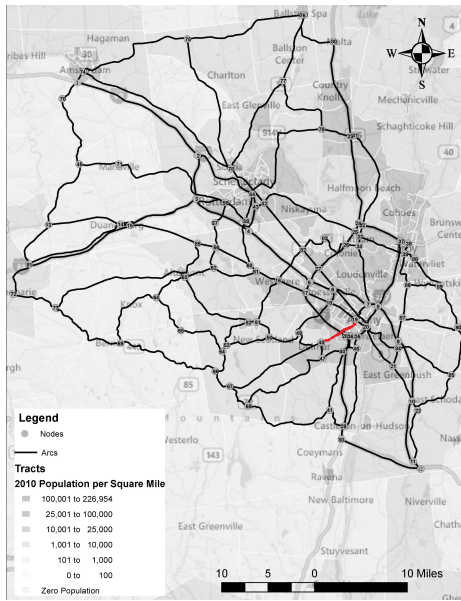
# WIM	Budget	Intercepted links
∞	∞	Opt. (4, 5), (61, 16), **(24, 25)**, **(33, 34)**, (80, 23), (42, 82), (5, 4), (16, 61), **(26, 25)**, **(33, 25)**, (51, 52), (44, 79), **(82, 42)**
		Pess. (4, 5), (61, 16), **(19, 20)**, **(27, 5)**, (80, 23), (42, 82), (5, 4), **(12, 11)**, (16, 61), **(27, 26)**, **(19, 7)**, **(35, 20)**, (51, 52), **(42, 43)**, (44, 79), **(42, 78)**
5	∞	Opt. (61, 16), (5, 4), (16, 61), (42, 43), (42, 78)
		Pess. (61, 16), (5, 4), (16, 61), (42, 43), (42, 78)
7	∞	Opt. (61, 16), (5, 4), (16, 61), **(26, 25)**, **(32, 24)**, **(33, 25)**, **(82, 42)**
		Pess. (61, 16), **(80, 23)**, (5, 4), (16, 61), **(51, 52)**, **(42, 43)**, **(42, 78)**
10	∞	Opt. (61, 16), (80, 23), (5, 4), (16, 61), (26, 25), (32, 24), (33, 25), (51, 52), **(44, 79)**, (82, 42)
		Pess. (61, 16), (80, 23), **(77, 78)**, (5, 4), (16, 61), (26, 25), (32, 24), (33, 25), (51, 52), (82, 42)
∞	3 m	Opt. (61, 16), **(24, 25)**, **(33, 34)**, **(37, 8)**, (78, 42), (5, 4), (16, 61), (26, 25), (33, 25), (51, 52), (82, 42)
		Pess. (61, 16), **(27, 5)**, **(80, 23)**, (78, 42), (5, 4), (16, 61), (26, 25), **(32, 24)**, (33, 25), (51, 52), (82, 42)
∞	5 m	Opt. (4, 5), (61, 16), (21, 10), (24, 25), **(5, 17)**, **(80, 23)**, **(42, 82)**, (5, 4), (16, 61), (26, 25), (33, 25), (48, 19), (51, 52), (44, 79), (82, 42)
		Pess. (4, 5), (61, 16), (21, 10), (24, 25), **(27, 5)**, **(43, 42)**, **(80, 23)**, **(78, 42)**, (5, 4), (16, 61), (26, 25), (33, 25), (48, 19), (51, 52), (44, 79), (82, 42)

of arcs, but also considering the population density, increase in the lengths of satisfying paths may not have a dominant effect.
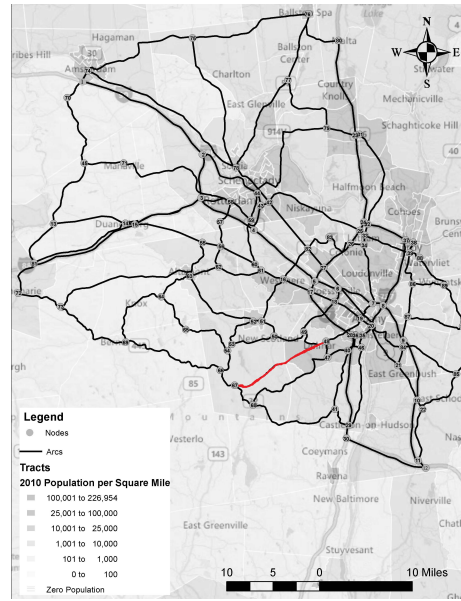
We investigate the effect of ϵ values on the locations of WIM systems. Figure 6b shows the total prevented damage cost to the network with respect to ϵ. We define the total prevented damage cost as damage costs of followers caused to the network in the absence of WIM stations. The total prevented damage cost increases up to $\epsilon = 30\%$ and decreases at $\epsilon = 40\%$. If we look at the detailed solution presented in Figure 7, we can see the differences of WIM locations under two different ϵ values. We marked the different locations only. Under $\epsilon = 30\%$, WIM systems are located in a shorter arc with higher population density compared to the solution with $\epsilon = 40\%$, which explains the decrease in the total prevented damage cost.

Another set of experiments investigates the location of WIM systems with constraints on the installation budget and the number of installations on the Albany network. The results are presented in Table 9. In all instances, except when the number of installations is set to 5, optimistic and pessimistic solutions result in different locations for WIM. When the number of installations is set to 5, both formulations select short links located in areas with a high density of population and consequently high damage costs. Figure 8 demonstrates the locations of WIM stations under

(a) $\epsilon = 30\%$ (b) $\epsilon = 40\%$
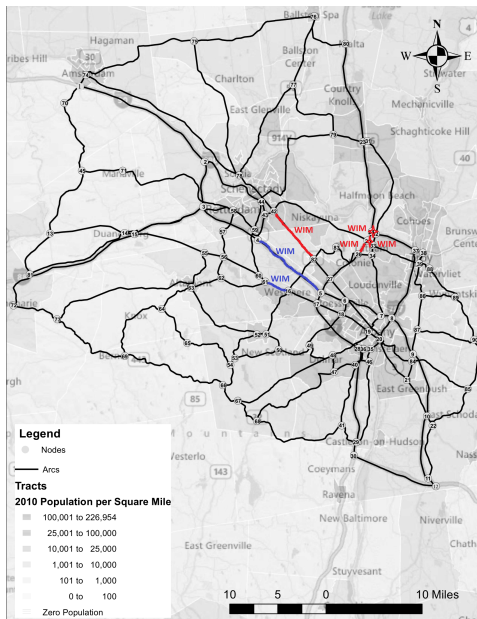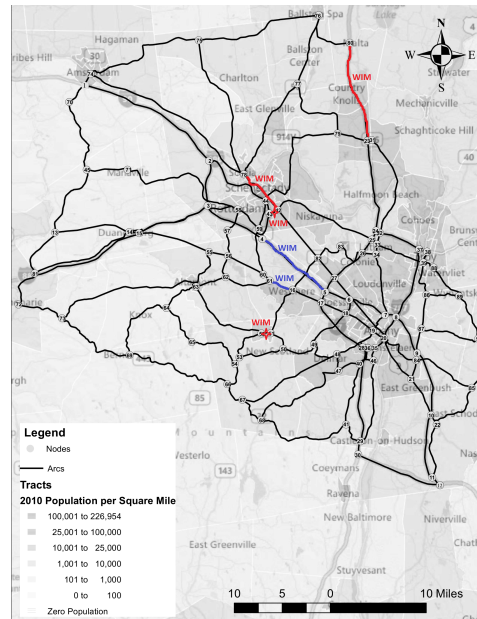
Figure 7: The differences of WIM locations for the Albany network using **PeBM$_\epsilon$**, $w_{ij} = \$360$k

(a) Optimistic   (b) Pessimistic

Figure 8: The differences of WIM locations for the Albany network using **PeBM$_\epsilon$**, $w_{ij} = \$260$k, with 7 installations. The common locations are shown in blue and own distinct locations are shown in red.

optimistic and pessimistic formulations, when the total number of installations cannot exceed 7.

7 Concluding Remarks

We present and solve the pessimistic formulations of the Evasive Flow Capturing Problem (EFCP), which aims to find efficient locations of law enforcement facilities in order to capture unlawful travelers. The proposed pessimistic formulations consider bounded rationality instead of perfect rationality in reactions of followers, thus representing more realistic behavior of travelers. Further, we let the followers select the most damaging paths, thus looking for the worst-case scenario for the decision of the leader.

To solve the resulting trilevel optimization problem, we propose a cutting plane algorithm to solve the problem exactly. The extensive computational studies confirm the efficiency of the proposed algorithm. We compare the solutions of the pessimistic formulations with those of optimistic approaches on the real and random networks. Depending on the cost of installation of the law enforcement facilities, the damage costs caused to a network by unlawful travelers under optimistic solutions may be up to 13.25% higher compared to pessimistic solutions on the Albany transportation network. While installations costs are typically high under the pessimistic solutions, they result in a long-term benefit in preserving the network infrastructure.

As a future research direction, novel solution methods can be developed to solve the pessimistic formulations on large networks. While the proposed pessimistic formulations assume ambiguity among satisfying paths, the future models may consider uncertainty in the threshold for calculations of the lengths of satisfying paths.

Acknowledgement

Appendix

A   Proofs of Statements

Proof of Proposition 1. If $\widehat{u}_f = 0$, then $\widehat{\mathbf{r}}^f = 0$; hence it is trivial. For any $\boldsymbol{\sigma}^f \in \boldsymbol{\Sigma}^f$, we first note that

$$(\bar{\lambda}_f + \delta)\widehat{u}_f - \sum_{(i,j)\in\mathcal{A}_f} (d_{ij} + \sigma_{ij}^f)\widehat{r}_{ij}^f \geq 0,$$

since the objective function value is 0 when $\widehat{u}_f = 0$. Suppose $\widehat{u}_f = 1$. Then we have

$$\sum_{(i,j)\in\mathcal{A}_f} (d_{ij} + \sigma_{ij}^f)\widehat{r}_{ij}^f \leq (\bar{\lambda}_f + \delta)\widehat{u}_f$$

which leads to

$$\sum_{(i,j)\in\mathcal{A}_f} d_{ij}\widehat{r}_{ij}^f \leq (\bar{\lambda}_f + \delta) - \sum_{(i,j)\in\mathcal{A}_f} \sigma_{ij}^f\widehat{r}_{ij}^f$$

$$\leq \bar{\lambda}_f + \delta,$$

since $\sigma_{ij}^f \geq 0$. Finally, we obtain $\sum_{(i,j)\in\mathcal{A}_f} d_{ij}\widehat{r}_{ij}^f \leq \bar{\lambda}_f$, since $\delta < d_{ij}$ for all $(i,j) \in \mathcal{A}^f$. $\qquad\square$

Proof of Proposition 2. We observe that

$$(\bar{\lambda}_f + \delta)\widehat{u}_f - \sum_{(i,j)\in\mathcal{A}_f} (d_{ij} + \widehat{\sigma}_{ij}^f)\widehat{r}_{ij}^f = (\bar{\lambda}_f + \delta)\widehat{u}_f - \sum_{(i,j)\in\mathcal{A}_f} d_{ij}\widehat{r}_{ij}^f$$

$$\geq 0$$

$$\geq (\bar{\lambda}_f + \delta)u_f - \sum_{(i,j)\in\mathcal{A}_f} (d_{ij} + \widehat{\sigma}_{ij}^f)r_{ij}^f$$

for all $(\mathbf{r}^f, u_f) \in \mathbf{L}^f(\bar{\mathbf{x}})$. Therefore, we obtain the proposition. $\qquad\square$

Proof of Proposition 3. If $\widehat{u}_f = 0$, then $\widehat{\mathbf{r}}^f = 0$; hence the results are trivial. We only consider the cases with $\widehat{u}_f = 1$.

(i) For any $\sigma^f \in \mathbf{\Sigma}_{\boldsymbol{\epsilon}}^f$, we first note that

$$\frac{\bar{\lambda}_f + \delta}{1 + \epsilon_f}\widehat{u}_f - \sum_{(i,j)\in\mathcal{A}_f} (d_{ij} - \sigma_{ij}^f)\widehat{r}_{ij}^f \geq 0,$$

since the objective function value is 0 when $\widehat{u}_f = 0$. With $\widehat{u}_f = 1$, we have

$$\sum_{(i,j)\in\mathcal{A}_f} d_{ij}\widehat{r}_{ij}^f \leq \frac{\bar{\lambda}_f + \delta}{1 + \epsilon_f} + \sum_{(i,j)\in\mathcal{A}_f} \sigma_{ij}^f\widehat{r}_{ij}^f \qquad (61)$$

Since $0 \leq \sigma_{ij}^f \leq \frac{\epsilon_f}{1 + \epsilon_f}d_{ij}$, (61) should be true when $\sigma_{ij}^f = 0 \quad \forall(i,j) \in \mathcal{A}_f$. Then, we have

$$\sum_{(i,j)\in\mathcal{A}_f} d_{ij}\widehat{r}_{ij}^f \leq \frac{\bar{\lambda}_f + \delta}{1 + \epsilon_f} \leq \bar{\lambda}_f + \delta,$$

which is equivalent to $\sum_{(i,j)\in\mathcal{A}_f} d_{ij}\widehat{r}_{ij}^f \leq \bar{\lambda}_f$.

(ii) Since $\widehat{u}_f = 1$, the problem in $\mathfrak{L}_{\boldsymbol{\epsilon}}^f(\mathbf{x}; -\boldsymbol{\sigma}^f)$ is equivalent to the minimization of $\sum_{(i,j)\in\mathcal{A}_f} (d_{ij} -$

$\sigma_{ij}^f)r_{ij}^f$, for which $\widehat{\mathbf{r}}^f$ is an optimal solution. Observe that:

$$\sum_{(i,j)\in\mathcal{A}_f} (d_{ij} - \sigma_{ij}^f)\widehat{r}_{ij}^f \leq \sum_{(i,j)\in\mathcal{A}_f} (d_{ij} - \sigma_{ij}^f)\mathring{r}_{ij}^f \leq \sum_{(i,j)\in\mathcal{A}_f} d_{ij}\mathring{r}_{ij}^f,$$

since $\sigma_{ij}^f \geq 0$ for all $(i,j) \in \mathcal{A}_f$. We also have

$$\sum_{(i,j)\in\mathcal{A}_f} \left(d_{ij} - \frac{\epsilon_f}{1+\epsilon_f}d_{ij}\right)\widehat{r}_{ij}^f \leq \sum_{(i,j)\in\mathcal{A}_f} (d_{ij} - \sigma_{ij}^f)\widehat{r}_{ij}^f \leq \sum_{(i,j)\in\mathcal{A}_f} d_{ij}\mathring{r}_{ij}^f,$$

since $\sigma_{ij}^f \leq \frac{\epsilon_f}{1+\epsilon_f}d_{ij}$ for all $(i,j) \in \mathcal{A}_f$. Consequently, we have

$$\sum_{(i,j)\in\mathcal{A}_f} d_{ij}\widehat{r}_{ij}^f \leq (1+\epsilon_f) \sum_{(i,j)\in\mathcal{A}_f} d_{ij}\mathring{r}_{ij}^f.$$

Hence we obtain the proposition. $\qquad\square$

Proof of Proposition 4. The proposition is true for more general cases; for all $(\widehat{\mathbf{r}}^f, \widehat{u}_f) \in \mathbf{L}^f(\mathbf{x})$ such that $\sum_{(i,j)\in\mathcal{A}_f} d_{ij}\widehat{r}_{ij}^f \leq \sum_{(i,j)\in\mathcal{A}_f} d_{ij}\mathring{r}_{ij}^f(1+\epsilon_f)$. With $\widehat{u}_f = 1$, the problem in $\mathfrak{L}_\epsilon^f(\mathbf{x}; -\boldsymbol{\sigma}^f)$ is equivalent to the minimization of $\sum_{(i,j)\in\mathcal{A}_f}(d_{ij} - \sigma_{ij}^f)r_{ij}^f$. By applying Theorem 6 of Sun et al. (2018), we complete the proof. $\qquad\square$

Proof of Proposition 5. Let $(\mathbf{x}^*, \mathbf{r}^*, \mathbf{u}^*)$ be optimal to **PeBM**. That is,

$$(\mathbf{r}^{f*}, u_f) = \underset{(\mathbf{r}^f, u_f)\in\mathbb{L}_f(\mathbf{x}^*)}{\arg\max} \sum_{(i,j)\in\mathcal{A}} h_{ij}r_{ij}^f. \tag{62}$$

for each $f \in \mathcal{F}$. We need to show that the above optimal solution satisfies both cuts (26) and (27). We prove by induction. In the first iteration, when no cuts are added, the proposition is obviously true.

In iteration $k-1$, we assume that the proposition is true. When the master solution $(\bar{\mathbf{x}}, \bar{\mathbf{r}}, \bar{\mathbf{u}})$ and the WCP solution $(\widehat{\mathbf{r}}, \widehat{\mathbf{u}})$ are obtained, distinct subpaths $\bar{p}$ and $\widehat{p}$ are identified, and new cuts are generated and added to the master problem in iteration k. We show that these new cuts (26) and (27) do not cut out the optimal solution. For each flow $f \in \mathcal{F}$, we consider two cases: $u_f^* = 0$ and $u_f^* = 1$.

(i) When $u_f^* = 0$, we also have $\mathbf{r}^{f*} = \mathbf{0}$. Therefore, (26) is trivially satisfied at the optimal solution. To show that $\mathbf{x}^*$ and u_f^* also satisfy (27), we suppose not. That is, we assume

$$\sum_{(i,j)\in\widehat{p}} x_{ij}^* \not\geq 1 - u_f^* = 1,$$

28

which implies $\sum_{(i,j)\in\widehat{p}} x_{ij}^* = 0$. Cut (27) was added in iteration $k-1$, because we had $\bar{u}_f = 0$; therefore $\widehat{p}$ implies a complete path from the origin to the destination for flow f. Since path $\widehat{p}$ is unintercepted and available for traveling, we observe that $u_f^* = 0$ cannot be optimal to WCP in (62).

(ii) When $u_f^* = 1$, (27) is trivially satisfied at the optimal solution. To show that $\mathbf{x}^*$ and u_f^* also satisfy (26), we need to show

$$\sum_{(i,j)\in\widehat{p}} x_{ij}^* \geq 1 - |\bar{p}| + \sum_{(i,j)\in\bar{p}} r_{ij}^{f*}. \tag{63}$$

Consider two subcases. If $\sum_{(i,j)\in\bar{p}} r_{ij}^{f*} < |\bar{p}|$, then (63) is satisfied. When $\sum_{(i,j)\in\bar{p}} r_{ij}^{f*} = |\bar{p}|$, subpath $\bar{p}$ is used by $\mathbf{r}^{f*}$. That is, subpath $\bar{p}$ is part of the WCP solution in (62). Let us suppose (63) does not hold. That is, we assume

$$\sum_{(i,j)\in\widehat{p}} x_{ij}^* \not\geq 1 - |\bar{p}| + \sum_{(i,j)\in\bar{p}} r_{ij}^{f*} = 1,$$

which implies $\sum_{(i,j)\in\widehat{p}} x_{ij}^* = 0$. Note that subpath $\widehat{p}$ was part of the unique optimal solution to WCP in iteration $k-1$. That is, $\sum_{(i,j)\in\bar{p}} h_{ij} < \sum_{(i,j)\in\widehat{p}} h_{ij}$. Since subpath $\widehat{p}$ is unintercepted by $\mathbf{x}^*$ and available for traveling, subpath $\bar{p}$ cannot be part of the optimal solution to WCP in (62). $\qquad\square$

Proof of Proposition 6. We first note that Corollary 1 enables us to change the variable $\boldsymbol{\sigma}$ in (30)–(35) by a new binary variable $\mathbf{y}$ such that $y_{ij}^f = 1 - r_{ij}^f$ and, subsequently, $y_{ij}^f r_{ij}^f = 0$ for all $f \in \mathcal{F}$ and $(i,j) \in \mathcal{A}_f$. We use inequalities $y_{ij}^f r_{ij}^f \leq 0$ in the constraints; similarly for (39), we use $\bar{x}_{ij}^f r_{ij}^f \leq 0$, which in combination leads to $(\bar{x}_{ij}^f + y_{ij}^f) r_{ij}^f \leq 0$. We obtain:

$$\underset{\mathbf{y}^f}{\text{maximize}} \quad \sum_{(i,j)\in\mathcal{A}_f} h_{ij}^f r_{ij}^f \tag{64}$$

$$\text{subject to} \quad y_{ij}^f \in \{0,1\} \qquad \forall (i,j) \in \mathcal{A}_f \tag{65}$$

$$\underset{\mathbf{r}^f, u_f}{\text{maximize}} \quad (\bar{\lambda}_f + \delta) u_f - \sum_{(i,j)\in\mathcal{A}_f} d_{ij} r_{ij}^f \tag{66}$$

$$\text{subject to} \quad \sum_{(i,j)\in\mathcal{A}_f} r_{ij}^f - \sum_{(j,i)\in\mathcal{A}_f} r_{ji}^f \leq \begin{cases} u_f & \text{if } i = s_f \\ -u_f & \text{if } i = t_f \\ 0 & \text{otherwise} \end{cases} \qquad \forall i \in \mathcal{N}_f \qquad (\pi_i^f) \tag{67}$$

$$(\bar{x}_{ij} + y_{ij}^f) r_{ij}^f \leq 0 \qquad\qquad\qquad \forall (i,j) \in \mathcal{A}_f \qquad (\nu_{ij}^f) \tag{68}$$

$$u_f \leq 1 \qquad\qquad\qquad\qquad (\eta_f) \tag{69}$$

$$u_f, r_{ij}^f \geq 0 \qquad\qquad\qquad\qquad \forall (i,j) \in \mathcal{A}_f \tag{70}$$

for each $f \in \mathcal{F}$. Note that the integrality of u_f and $\mathbf{r}^f$ is relaxed, since the lower-level problem

satisfies the total unimodularity, and the inequality form in (67) is used. Using the dual variables $\boldsymbol{\pi}^f$ and η_f, the dual problem can be written as:

$$\underset{\boldsymbol{\pi}^f, \boldsymbol{\nu}^f, \eta_f}{\text{minimize}} \quad \eta_f \tag{71}$$

$$\text{subject to} \quad \pi_i^f - \pi_j^f + \mu_{ij}^f(\bar{x}_{ij} + y_{ij}^f) + d_{ij} \geq 0 \qquad \forall (i,j) \in \mathcal{A}_f \tag{72}$$

$$\pi_{t_f}^f - \pi_{s_f}^f + \eta^f \geq \bar{\lambda}_f + \delta \tag{73}$$

$$\eta_f, \pi_k^f, \mu_{ij}^f \geq 0 \qquad \forall k \in \mathcal{N}_f, (i,j) \in \mathcal{A}_f \tag{74}$$

for each $f \in \mathcal{F}$. Note that the lower-level problem of the above bilevel problem is identical in its structure to the lower-level problem of the optimistic formulation considered in Arslan et al. (2018). Using Proposition 1 of Arslan et al. (2018), we can show that there exists an optimal solution to (71)–(74) such that $\mu_{ij}^f = \bar{\lambda}_f + \delta$ for all $(i,j) \in \mathcal{A}_f$. By replacing the lower-level by its optimality conditions and eliminating η_f by using strong duality, we obtain (37)–(44). $\qquad \square$

Proof of Proposition 7. It can be proved similar to Proposition 6. The dual problem of the lower-level can be written as follows:

$$\text{minimize} \quad \eta^f \tag{75}$$

$$\text{subject to} \quad \pi_i^f - \pi_j^f + \mu_{ij}^f \bar{x}_{ij} + (d_{ij} - \sigma_{ij}^f) \geq 0 \tag{76}$$

$$\pi_{t_f}^f - \pi_{s_f}^f + \eta^f \geq \frac{\bar{\lambda}_f + \delta}{1 + \epsilon_f} \tag{77}$$

$$\eta^f, \pi_i^f, \mu_{ij}^f \geq 0 \tag{78}$$

Using Proposition 1 of Arslan et al. (2018), we can show that there exists an optimal solution such that $\mu_{ij}^f = \bar{\lambda}_{ij} + \delta$. With the strong duality, we have

$$\eta^f = \frac{\bar{\lambda}_f + \delta}{1 + \epsilon_f} u_f - \sum_{(i,j) \in \mathcal{A}_f} (d_{ij} - \sigma_{ij}^f) r_{ij}^f \tag{79}$$

Eliminating η^f using (79) in the dual feasibility constraints (77) and (78), we obtain the following conditions respectively:

$$\frac{\bar{\lambda}_f + \delta}{1 + \epsilon_f}(1 - u_f) + \sum_{(i,j) \in \mathcal{A}_f} (d_{ij} - \sigma_{ij}^f) r_{ij}^f \leq \pi_{t_f}^f - \pi_{s_f}^f \tag{80}$$

$$\frac{\bar{\lambda}_f + \delta}{1 + \epsilon_f} u_f - \sum_{(i,j) \in \mathcal{A}_f} (d_{ij} - \sigma_{ij}^f) r_{ij}^f \geq 0. \tag{81}$$

By using (20) in Proposition 4, we can let $\sigma_{ij}^f = \dfrac{\epsilon_f}{1 + \epsilon_f} d_{ij} r_{ij}^f$ and rewrite (80) and (81) as (55) and

(56), respectively. □

References

Arslan, O., O. Jabali, G. Laporte. 2018. Exact solution of the evasive flow capturing problem. *Operations Research* **66**(6) 1625–1640.

Berman, O., D. Bertsimas, R. C. Larson. 1995. Locating discretionary service facilities, II: maximizing market size, minimizing inconvenience. *Operations Research* **43**(4) 623–632.

Berman, O., R. C. Larson, N. Fouska. 1992. Optimal location of discretionary service facilities. *Transportation Science* **26**(3) 201–211.

Bromberger, S., J. Fairbanks, other contributors. 2017. JuliaGraphs/LightGraphs.jl: LightGraphs. doi:10.5281/zenodo.889971.

Cottrell, B. H., et al. 1992. The avoidance of weigh stations in Virginia by overweight trucks. Tech. rep., Virginia Transportation Research Council.

Cunagin, W., W. Mickler, C. Wright. 1997. Evasion of weight-enforcement stations by trucks. *Transportation Research Record* **1570**(1) 181–190.

Dey, K. C., M. Chowdhury, W. Pang, B. J. Putman, L. Chen. 2014. Estimation of pavement and bridge damage costs caused by overweight trucks. *Transportation Research Record* **2411**(1) 62–71.

Erdoğan, S., E. Miller-Hooks. 2012. A green vehicle routing problem. *Transportation Research Part E: Logistics and Transportation Review* **48**(1) 100–114.

Fontaine, P., T. G. Crainic, M. Gendreau, S. Minner. 2020. Population-based risk equilibration for the multimode hazmat transport network design problem. *European Journal of Operational Research* **284**(1) 188–200.

Fontaine, P., S. Minner. 2018. Benders decomposition for the hazmat transport network design problem. *European Journal of Operational Research* **267**(3) 996–1002.

Gzara, F. 2013. A cutting plane approach for bilevel hazardous material transport network design. *Operations Research Letters* **41**(1) 40–46.

Hodgson, M. J. 1990. A flow-capturing location-allocation model. *Geographical Analysis* **22**(3) 270–279.

Hodgson, M. J., K. E. Rosing, J. Zhang. 1996. Locating vehicle inspection stations to protect a transportation network. *Geographical Analysis* **28**(4) 299–314.

Hooshmand, F., S. MirHassani. 2018. An effective bilevel programming approach for the evasive flow capturing location problem. *Networks and Spatial Economics* 1–27.

Irnich, S., D. Villeneuve. 2006. The shortest-path problem with resource constraints and k-cycle elimination for $k \geq 3$. *INFORMS Journal on Computing* **18**(3) 391–406.

Kang, Y., R. Batta, C. Kwon. 2014a. Generalized route planning model for hazardous material transportation with var and equity considerations. *Computers & Operations Research* **43** 237–247.

Kang, Y., R. Batta, C. Kwon. 2014b. Value-at-risk model for hazardous material transportation. *Annals of Operations Research* **222**(1) 361–387.

Kara, B. Y., V. Verter. 2004. Designing a road network for hazardous materials transportation. *Transportation Science* **38**(2) 188–196.

Kim, J.-G., M. Kuby. 2012. The deviation-flow refueling location model for optimizing a network of refueling stations. *International Journal of Hydrogen Energy* **37**(6) 5406–5420.

Liu, X., C. Kwon. 2020. Exact robust solutions to the combined facility location and network design for hazardous materials. *IISE Transactions* **52**(10) 1156–1172. URL `https://doi.org/10.1080/24725854.2019.1697017`.

Lozano, L., D. Duque, A. L. Medaglia. 2015. An exact algorithm for the elementary shortest path problem with resource constraints. *Transportation Science* **50**(1) 348–357.

Lu, C.-C., S. Yan, H.-C. Ko, H.-J. Chen. 2017. A bilevel model with a solution algorithm for locating weigh-in-motion stations. *IEEE Transactions on Intelligent Transportation Systems* **19**(2) 380–389.

Lu, Q., J. Harvey, T. Le, J. Lea, R. Quinley, D. Redo, J. Avis. 2002. Truck traffic analysis using weigh-in-motion (WIM) data in California. Tech. rep., Report produced under the auspices of the California Partnered Pavement Research Program for the California Department of Transportation Pavement Research Center, Institute of Transportation Studies, University of California, Berkeley.

Mahmassani, H. S., G.-L. Chang. 1987. On boundedly rational user equilibrium in transportation systems. *Transportation Science* **21**(2) 89–99.

Marković, N., I. O. Ryzhov, P. Schonfeld. 2015. Evasive flow capture: Optimal location of weigh-in-motion systems, tollbooths, and security checkpoints. *Networks* **65**(1) 22–42.

Marković, N., I. O. Ryzhov, P. Schonfeld. 2017. Evasive flow capture: A multi-period stochastic facility location problem with independent demand. *European Journal of Operational Research* **257**(2) 687–703.

Martin, A., V. J. Keathley, J. Kissick, J. R. Walton. 2014. Coordinating the use and location of weigh-in-motion technology for Kentucky. Tech. rep., Kentucky Transportation Center Research Report. 1416.

Nakayama, S., R. Kitamura, S. Fujii. 2001. Drivers' route choice rules and network behavior: Do drivers become rational and homogeneous through learning? *Transportation Research Record: Journal of the Transportation Research Board* (1752) 62–68.

Reagor, D. M. 2002. An evaluation of Montana's State Truck Activities Reporting System (STARS). Ph.D. thesis, Montana State University-Bozeman, College of Engineering.

Schneider, M., A. Stenger, D. Goeke. 2014. The electric vehicle-routing problem with time windows and recharging stations. *Transportation Science* **48**(4) 500–520.

Sinha, A., P. Malo, K. Deb. 2018. A review on bilevel optimization: from classical to evolutionary approaches and applications. *IEEE Transactions on Evolutionary Computation* **22**(2) 276–295.

Song, Y., S. Shen. 2016. Risk-averse shortest path interdiction. *INFORMS Journal on Computing* **28**(3) 527–539.

Su, L., C. Kwon. 2020. Risk-averse network design with behavioral conditional value-at-risk for hazardous materials transportation. *Transportation Science* **54**(1) 184–203.

Sun, L., M. H. Karwan, C. Kwon. 2015. Robust hazmat network design problems considering risk uncertainty. *Transportation Science* **50**(4) 1188–1203.

Sun, L., M. H. Karwan, C. Kwon. 2018. Generalized bounded rationality and robust multicommodity network design. *Operations Research* **66**(1) 42–57.

Szary, P. J., A. Maher, et al. 2009. Implementation of weigh-in-motion (WIM) systems. Tech. rep., New Jersey. Dept. of Transportation.

Wiesemann, W., A. Tsoukalas, P.-M. Kleniati, B. Rustem. 2013. Pessimistic bilevel optimization. *SIAM Journal on Optimization* **23**(1) 353–380.

Yang, H., J. Zhou. 1998. Optimal traffic counting locations for origin–destination matrix estimation. *Transportation Research Part B: Methodological* **32**(2) 109–126.

Zare, M. H., O. Y. Özaltın, O. A. Prokopyev. 2018. On a class of bilevel linear mixed-integer programs in adversarial settings. *Journal of Global Optimization* **71**(1) 91–113.

Zhu, S., D. Levinson. 2015. Do people use the shortest path? An empirical test of Wardrop's first principle. *PloS ONE* **10**(8) e0134322.